SVERRE PETTERSSEN,
E. KNIGHTING, *R. W. JAMES*, AND *N. HERLOFSON*

CONVECTION IN THEORY AND PRACTICE

WITH 8 FIGURES IN THE TEXT

CONTENTS

ACKNOWLEDGEMENT

This paper was written during the war in response to a request by the Meteorological Office, British Air Ministry, for an investigation of the applicability of the instability criteria to the forecasting of convective currents and clouds.

My grateful thanks are due to the Director of the Meteorological Office for the excellent facilities and generous assistance afforded me during my war-time service in the Meteorological Office, and to the staff of the Upper Air Branch for their ever willing cooperation of which this paper is but one example.

Oslo, August 1945.

Sverre Petterssen.

CONVECTION IN THEORY AND PRACTICE

BY *SVERRE PETTERSSEN*,
E. KNIGHTING, *R. W. JAMES*, AND *N. HERLOFSON*

(Manuscript received September 7th, 1945)

I. INTRODUCTION

The vertical currents in the atmosphere may be classified according to their horizontal dimensions, viz.,

(1) *Turbulent eddies*, whose dimensions are of the order of magnitude of metres or tens of metres, and whose life is so short that the individual eddies do not normally become visible through the formation of clouds.

(2) *Convective currents*, whose dimensions are of the order of hundreds or thousands of metres, and whose life is of the order of a few hours. These currents will normally become visible through the formation of clouds in their ascending branches.

(3) *Large scale circulations*, whose dimensions are of the order of hundreds or thousands of kilometres (e.g. extratropical cyclones and anticyclones), and whose life is of the order of days. These circulations readily become visible through the formation of extensive cloud systems in their ascending branches.

The above classification does not represent a grouping according to arbitrary limits of what is small, medium, or large, for it is not observed that a turbulent eddy assumes the dimensions and characteristics of a cumulo-nimbus cloud, nor does a cumulo-nimbus cloud ever approach the dimensions of an extra-tropical cyclone. Thus, as far as horizontal dimensions are concerned, the convective currents stand out as a distinct type.

The vertical velocities associated with the above-mentioned currents are equally distinct. In the large scale circulations the vertical velocities are of the order of a few centimetres per second, whereas those associated with the convective currents are of the order of a few metres per second.

Amongst the numerous contributions to the theory of convection and to the technique of forecasting convective phenomena, only those which have a direct bearing on the present investigation will be mentioned here.

The first contribution to the theory of convection was rendered by Lord Kelvin (1865) who, by considering the compressibility of dry air, derived the expression for the dryadiabatic lapse rate. The next principal contribution is due to Hertz (1884) who, in addition to the compressibility, considered the liberation of the latent heat of vaporization, and developed an adiabatic chart with dry and saturated adiabatics, a diagram that was later perfected and introduced into synoptic practice by Stüve (1922).

Already during the later part of the First World War, Douglas (1920) studied convective phenomena, notably thunderstorms, and correlated their occurrence with the synoptic situations. Douglas' empirical results are of considerable interest, particularly since they show that the occurrence of thunderstorms is definitely related to the general synoptic situation.

Later investigations of convection have dealt mainly with the thermodynamical relationships, the criteria for static stability and instability, and the amount of energy available for the creation of convective currents. These investigations have resulted in two different methods of investigating convective phenomena, and two sets of criteria for stable and unstable stratifications. We shall refer to these methods as the Parcel Method and the Slice Method.

The parcel method, which is mainly due to Refsdal (1930) and Normand (1938), results from consideration of the buoyancy forces acting on a parcel of air that is displaced adiabatically in an undisturbed environment. The stability criteria thus obtained can be expressed in terms of lapse rate only, and the amount of energy available for the creation of convective currents can be obtained from a plot on an indicator diagram (e.g. a TePhi-gram).

The slice method, which was introduced by Bjerknes (1938) and extended by Petterssen (1939), is derived by considering the downward as well as the upward currents, having regard to the equation of continuity. The stability criteria thus derived, depend not only upon the lapse rate but also upon the kinematics of the motion. The expressions for the amounts of energy derived by the aid of the slice method differ essentially from those derived by the aid of the parcel method, the difference between the two amounts being proportional to the ratio of the ascending mass to the descending mass.

The essential difference between the parcel method and the slice method is that the adiabatic heating in the descending currents is neglected in the former and accounted for in the latter, with the result that in all cloud producing processes the parcel method renders amounts of energy, vertical acceleration and velocities that are much too large. The results derived by the aid of the slice method converge towards those derived by the aid of the parcel method when the horizontal dimensions of the ascending mass are small as compared with those of the descending mass.

The difficulty in the way of using the slice method in practice is due to the circumstance that the stability criteria and the amounts of available energy depend upon the ratio of the ascending mass to the descending mass, and since this ratio is not observed, only qualitative results can be obtained.

Regarding convection from a forecasting point of view, one would naturally desire criteria for: the commencement and cessation of convective currents, the vertical velocities and gusts, the vertical accelerations, the height of the base and of the top of the convective clouds, the cloud amount, and the release of precipitation. The aim of this investigation is to determine the practical applicability of the theories of convection to the analysis and forecasting of the said phenomena.

Section II of this paper contains a summary and, in certain respects, an extension of the present theories, with a formulation suitable for comparison with actual observations. About 300 aerological ascents and observations of clouds in convective situations have been analysed and compared with the theoretical relationships. The results are described in Section III, which also contains some statistical results relating the occurrence of convection to the synoptic situation, notably the vorticity of the large-scale currents.

II. SOME THEORETICAL RELATIONSHIPS

1. The Parcel Method: Stability Criteria.

The parcel method of investigating the stability of a stratification is based upon considerations of a parcel of air that is displaced adiabatically from its original position in such a manner that the environment remains undisturbed. The stratification is said to be stable, or unstable, according to whether the parcel becomes accelerated in the direction towards, or away from, the level whence it came.

We consider a parcel of air embedded in an environment that is in hydrostatic equilibrium, and let letters with indices refer to the parcel and letters without indices refer to the environment. Then:

$$\dot{w}' = -\alpha' \frac{\partial p'}{\partial z} - g$$
$$0 = -\alpha \frac{\partial p}{\partial z} - g \qquad (1)$$

Here,

$\dot{w}$ = vertical acceleration
α = specific volume
p = pressure
g = acceleration of gravity
z = distance along a vertical axis.

Since the pressure gradient along the vertical is determined by the surrounding air, we have

$$\frac{\partial p'}{\partial z} = \frac{\partial p}{\partial z}$$

and therefore,

$$\dot{w}' = g \frac{\alpha' - \alpha}{\alpha} \qquad (2)$$

or, from the equation of state

$$\dot{w}' = g \frac{T' - T}{T} \qquad (3)$$

where T = absolute temperature.

It will thus be seen that the parcel will be accelerated upwards if it is warmer, and downwards if it is colder, than the environment.

It is of interest to note that the only assumption made in the derivation of eq. (3) is that the air surrounding the parcel is not accelerated along the vertical; no assumption is made as regards adiabatic processes and vertical velocities.

If the horizontal distribution of temperature could be observed in sufficient detail, the static stability could be evaluated by the application of eq. (3). However, since the distance between the observing stations is large whereas the ascents give a continuous record of the temperature distribution along the vertical, it is more convenient to express the stability criteria in terms of the lapse rate of temperature.

We consider next a parcel of air at an arbitrary level z_0 where the temperature is T_0 and the lapse rate γ. Then

$$T = T_0 - \gamma \triangle z$$

describes the temperature along a vertical line through the point considered. If the parcel is displaced adiabatically a small distance $\triangle z$, its temperature will vary according to the adiabatic law, viz.,

$$T' = T_0 - \gamma_a \triangle z$$

If, during this displacement, the temperature of the environment remains unchanged,

$$T' - T = (\gamma - \gamma_a) \triangle z$$

and eq. (3) becomes

$$\dot{w}' = g \frac{\gamma - \gamma_a}{T} \triangle z \qquad (4)$$

which gives the stability criteria of the parcel method. It will be seen that the acceleration has the same sign as the displacement (i.e. instability) when

$$\gamma > \gamma_a$$

and its sign is opposite to that of the displacement (i.e. stability) when

$$\gamma < \gamma_a$$

Accordingly, the parcel method leads to the following criteria for stability and instability:

stable equilibrium: $\gamma < \gamma_a$
indifferent equilibrium: $\gamma = \gamma_a$
unstable equilibrium: $\gamma > \gamma_a$

In the above expressions, the dry-adiabatic (γ_d) or the saturated-adiabatic (γ_s) lapse rate should be used according to whether the parcel is non-saturated or saturated with moisture.

Although the equations (3) and (4) are similar in structure, there is a fundamental difference between the assumption underlying them.

Eq. (3) was derived on the sole assumption that the vertical acceleration is nil, or negligible. No assumption was made as regards the vertical velocity, nor were adiabatic changes introduced. The equation relates the *excess temperature* of the parcel to the acceleration relative to the environment, but it does not indicate how the excess temperature was established.

Eq. (4), on the other hand, was derived from eq. (3) on the basis of the additional assumptions that the motion of the parcel is adiabatic and that there is no vertical velocity in the environment. This latter assumption represents a severe restriction. We shall return to the discussion of this in a later paragraph. Here, it suffices to remark that eq. (4), and not eq. (3), expresses the contents of the parcel method. Eq. (4), however, represents a special case of eq. (3).

2. The Parcel Method: Energy, Velocity, and Acceleration.

The theory underlying the parcel method[1]) can be used to obtain some simple relationships between the vertical accelerations and velocities and the areas obtained from the plots on a TePhigram, or other diagrams which represent an equal-area transformation of the pressure-volume

[1]) The following discussion will refer to the theory of the parcel method as it is presented in standard meteorological texts, and not to the practice introduced by Sir Charles Normand and his associates in India by making plausible assumption as to the efficiency of the overturning processes.

diagram. The following discussion will refer to the Te-Phi-gram of the Meteorological Office, Air Ministry.

The vertical velocity of the parcel may be written

$$w' = \frac{dz}{dt}$$

and the acceleration

$$\dot{w}' = \frac{dw'}{dt}$$

Substitution into eq. (3) gives

$$\frac{d\left(\frac{1}{2}w'^2\right)}{d(gz)} = \frac{T'-T}{T} \qquad (5)$$

Since $(T' - T)$ is very small as compared with T, it follows that the variation in the kinetic energy is only a small fraction of the variation in the potential energy of the parcel.

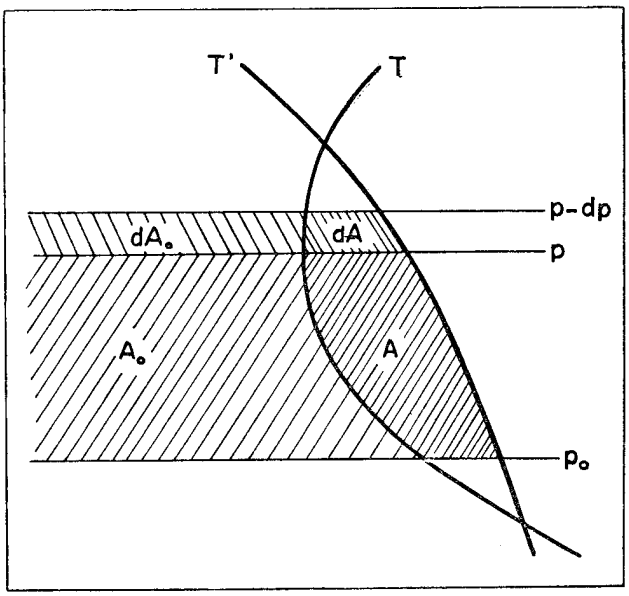

Fig. 1. — Schematical section of a TePhi-gram. T′ = temperature of the parcel; T = temperature of the environment. The area A_0 extends to the absolute zero.

We consider next Fig. 1 where T refers to the environment and T to the parcel. Let A_0 denote the area between two isobars to the left of the curve T and let A denote the area bounded by the same isobars and the curves T and T′. The TePhi-gram being an equal-area transformation of the pressure-volume diagram,

$$d(gz) = k dA_0 \qquad (6)$$

where k is the scale factor of the TePhi-gram relating area to energy.

On the TePhi-gram, the distance along an isotherm from one isobar to another is independent of the temperature, and from this it follows that

$$dA = \frac{T'-T}{T} dA_0 \qquad (7)$$

which combined with eqs. (5) and (6) gives

$$d\left(\tfrac{1}{2}w'^2\right) = k dA$$

and therefore

$$\tfrac{1}{2}w'^2 - \tfrac{1}{2}w'_0{}^2 = kA \qquad (8)$$

where A is measured from the isobar where the parcel was at the initial moment. It will be seen from eq. (7) that dA is positive when the parcel is warmer, and negative when the parcel is colder than the environment.

Solving with respect to the vertical velocity, we obtain:

$$w' = \sqrt{2\left(\tfrac{1}{2}w'_0{}^2 + kA\right)}$$

Now, in the TePhi-gram referred to above

$$k = \tfrac{1}{36}\,\frac{\text{Joule}}{\text{gm cm}^2}$$

and, when A is expressed in cm^2 and the velocity in m/sec

$$w' = \sqrt{w'_0{}^2 + \tfrac{1000}{18}A} \qquad (9)$$

If the vertical velocity is zero at the initial moment

$$w' = 7.45\sqrt{A} \qquad (10)$$

or

$$A = 0.018\, w'^2 \qquad (11)$$

On the other hand, if the initial velocity of the parcel is w'_0, it can describe the negative area

$$A = -0.018\, w'_0{}^2 \qquad (12)$$

before its kinetic energy is consumed.

We shall return to these relationships in connection with the discussion of the statistical results in Section III.

3. The Parcel Method: Normand's Classification.

For the following investigation it is of interest to recapitulate the essential features of the parcel method and summarize the classification of the

various types of stratifications. Following Normand, we consider a TePhi-gram in which are plotted the ascent curves of temperature T and wet-bulb temperature T_w, as shown diagrammatically in Fig. 2.

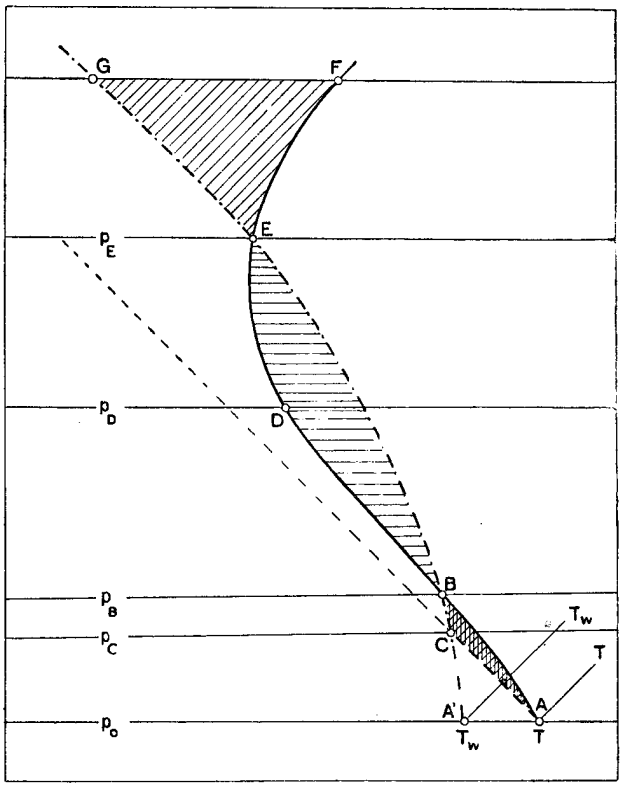

Fig. 2. — Schematical plot on a TePhi-gram. The curve ABDEF represents the temperature, and the curve A'BEG the saturated-adiabatic through the wet-bulb temperature point T_w. The area ACB is the lower negative area, BDEB is the positive area, and EGF the upper negative area. The point C is the condensation level of the parcel at A. At the level D the lapse rate is equal to the saturated-adiabatic rate.

To illustrate the application of the parcel method to actual ascents, we consider a parcel of air at an arbitrary level, say A, where the temperature is T and the wet-bulb temperature is T_w. If the parcel is displaced upwards, it will cool dry-adiabatically and become saturated at the level C, (i.e. on the isobar p_c) whence it cools at the saturated-adiabatic rate.

During its ascending motion, from A to B, the parcel will be colder than the environment and, therefore, be accelerated downwards, i. e. against its displacement. The area ABC in Fig. 2 represents the amount of energy that must be supplied to a parcel of unit mass at A in order to overcome the buoyancy forces and bring the parcel to the level B, or the isobar p_B. We shall refer to this area as the *negative area.*

If the parcel at A is lifted beyond the level B, it will become warmer than the environment and, therefore, be accelerated in the direction of its displacement. The parcel would ascend further and continue to be accelerated until it reaches the level E, where its temperature would be equal to that of its environment. The area BDEB on the TePhi-gram represents the amount of energy gained by the parcel while it moves from the level B to the level E, and this area would represent the kinetic energy of the parcel as it arrives at the level E. We shall refer to this area as the *positive area.*

The amount of kinetic energy gained by the parcel while ascending to the level E must now be expended above the level E, and the parcel would ascend to some level G, such that the negative area EGF equals the amount of kinetic energy possessed by the parcel when it passed the level E. We shall refer to this area as the *upper negative area.*

The above represents the essence of the parcel method of investigating the stability of a stratification.

It will be seen that the amounts of energy, or the size of the areas, depend not only upon the lapse rates but also upon the degree of saturation. Thus, for example, the negative area (ACB) in Fig. 2 will decrease as the lapse rate from A to B increases, and it will also decrease if the wet-bulb temperature at the level A increases. An increase in the wet-bulb temperature at the level A would not only reduce the negative area but also greatly increase the positive area.

On the above principles, Normand classified the various types of stratifications according to the relative size of the positive and negative areas. If N denotes the magnitude of the lower negative area (see Fig. 2) and P the magnitude of the positive area, Normand's classification may be summarised as follows.

1. *Absolute stability*, characterised by
$$N > 0 \quad \text{and} \quad P = 0$$
2. *Absolute instability*, characterised by
$$N = 0 \quad \text{and} \quad P > 0$$

3. *Conditional instability*, characterised by

$$N > 0 \quad \text{and} \quad P > 0$$

This case may be subdivided into two classes, viz.,

(a) *Real latent type*, characterised by

$$P > N$$

In this case the amount of energy, that must be supplied to a parcel of unit mass at A in Fig. 2, is less than the amount of energy that can be released above the level B. The difference

$$P - N$$

is taken to represent the amount of energy available for the creation of convective currents.

(b) *Pseudo-latent type*, characterised by

$$P < N$$

In this case

$$P - N < 0$$

and there is no net amount of energy available for the creation of convective currents.

With regard to Normand's classification it is of interest to note that the criteria for absolute stability and absolute instability are in agreement with eqs. (3) and (4). The same is not true of the criteria referred to under the heading of Conditional Instability, for if there is a negative area, the displaced parcel will be colder than the environment, and will, therefore, be accelerated towards its level of origin. In this connection the difference in size of the positive and the negative areas is immaterial, for the energy represented by the positive area cannot be made available unless the negative area has been eliminated.

The possibility exists that the parcel (in spite of the negative area) could move from the level A to the level B (Fig. 2) as a result of an external impulse. The magnitude of this impulse is readily assessed. Suppose that the negative area on the TePhi-gram were as small as 1 cm². It will then be seen from eq. (12) that the parcel must be given an initial velocity of 7.5 m/sec to enable it to reach the level B where it could begin to benefit by the energy represented by the positive area. Even if the negative area were as small as 1.8 mm² (which is imperceptable on the TePhi-gram), the initial vertical velocity would have to be 1 m/sec for the parcel to move through the negative area. It will thus be seen that the positive area does not constitute a source of energy unless the negative area has been eliminated or reduced to an immeasurable size.

Nevertheless, when the negative area of the air at the earth's surface (as shown by the ascent curve) is very small, the negative area is likely to be non-existent locally (over super-heated areas), with the result that, on the average, there is a certain probability for convective currents to be released, and this probability increases as the negative area (as shown by representative temperature observations) approaches zero. As will be shown in Section III, convective currents are likely to be released as soon as the negative area becomes less than 0.5 cm². This, however, does not imply that convective currents can be released by mechanical impulses and force their way through a negative area of this size; it only implies that when the representative temperatur curve shows a negative area less than 0.5 cm², the area is likely to be absent locally. As the heating continues, the negative area disappears generally, and convection becomes widespread.

4. The Parcel Method: Cloud Base, Top, and Amount.

The assumptions underlying the parcel method lead to some definite relations between the ascent curve and the levels at which the base and the top of the convective cloud should be found.

1. *The condensation level* is obtained from the ascent curve as follows. Let A in Fig. 2 represent the temperature and A′ the wet-bulb temperature of a parcel of air near the earth's surface. If the parcel is lifted adiabatically with constant moisture content, its temperature point will follow the dry-adiabatic through A, and its wet-bulb temperature point will follow the saturated-adiabatic through A′. The condensation level is then the point of intersection of these two adiabatics. The condensation level, thus determined, refers to convection that starts from the earth's surface. In rare cases,[1]) convection

[1]) The qualification «rare» refers to the observational material examined. In tropical and sub-tropical regions, convective instability is often present, and convection is released aloft.

may be released from some higher level, in which case the temperature and the wet-bulb temperature at the appropriate level must be considered.

The discussion in the following paragraphs will be limited to convective currents which commence at, or near, the earth's surface. The success that can be obtained by evaluating the condensation level, as described above, will largely depend upon the extent to which the moisture content of the ascending air is conserved, or, in other words, the amount of mixing between the ascending currents and the environment. A statistical comparison between the computed condensation level and the observed cloud base will be given in Section III.

2. *The top of convective clouds.* According to the parcel method, the ascending air would rise on account of the buoyancy forces above the level B in Fig. 2, and arrive at the level E with a maximum of kinetic energy. Above the level E, the motion would be retarded and the parcel would continue to the top of the upper negative area, i.e. to G in Fig. 2. Accordingly, the tops of convective clouds would be observed at, or near, the top of the upper negative area. As will be shown in Section III, the observed cloud tops rarely reach above the level D in Fig. 2, showing that there is a vast difference between the computed and the observed heights to which the convective clouds reach.

3. *Cloud amount.* The environment being undisturbed, the parcel method renders no upper limit to the amounts of convective cloud, and no relation between the cloud amount and the ascent curve.

5. The Parcel Method: Magnitude of Velocities and Accelerations.

The magnitude and the distribution of the vertical velocities and accelerations that would result from the parcel method, are readily obtained from the ascent curves. We return to Fig. 2 and consider a parcel of air at the lower end of the positive area, i.e. at B, where the initial vertical velocity is supposed to be negligible. As soon as the parcel is displaced beyond this level, acceleration sets in, and the acceleration reaches a maximum value at the level D, where the temperature difference between the parcel and the environment reaches a maximum value. However, the acceleration continues until the parcel reaches the level E, i.e. the top of the positive area. Here, then, the vertical velocity reaches its highest value. These conclusions will be discussed in relation to observational evidence in Section III. What we are here concerned to show is the numerical relations between the areas obtained from the analysis of the TePhi-gram and the vertical velocities that would be observed if the parcel method were reasonably accurate.

Table A shows the vertical accelerations computed from eq. (3) for various values of T′ and T.

Table B is computed from eq. (4) for various deviations of the actual lapse rate from the appropriate adiabatic rate.

Table C, which is computed from eq. (11), shows the vertical velocity of the parcel after it has described a positive area of the indicated size. This table will be used in Section III in connection with the statistical analysis of the areas obtained from the TePhi-grams in a large number of convective situations.

Table A.

Vertical Accelerations (m/sec²) computed from Equation 3.

T°C	T′—T (°C)				
	± 1	± 5	± 10	± 15	± 20
— 30	± 0.04	± 0.20	± 0.40	± 0.60	± 0.81
0	± 0.04	± 0.18	± 0.36	± 0.54	± 0.72
+ 30	± 0.03	± 0.16	± 0.32	± 0.49	± 0.65

Table B.

Vertical Accelerations (m/sec²) computed from Equation 4 for a Displacement of 100 metres.

T°C	$\gamma - \gamma_a$ (°C per 100 m)				
	— 3	— 2	— 1	0	0.5
— 30	— 0.12	— 0.08	— 0.04	0	0.020
0	— 0.11	— 0.07	— 0.04	0	0.018
+ 30	— 0.10	— 0.06	— 0.03	0	0.016

Table C.

Vertical Velocities (m/sec) corresponding to Areas (cm²) on the TePhi-gram, computed from Equation 11.

Vertical Velocity m/sec	Area cm²
1	0.02
2	0.07
5	0.45
10	1.80
15	4.05
20	7.20
30	16.20
40	28.80
50	45.00

In connection with Table C it is of interest to note that the most frequent size of the positive area in convective situations is about 15 cm² to which corresponds, according to the parcel method, a vertical velocity at the top of the positive area of about 30 m/sec. In extreme cases positive areas as large as 60 cm² have been observed, to which would correspond a vertical velocity of about 60 m/sec.

6. The Slice Method: Stability Criteria.

In the foregoing paragraphs we considered a parcel of air mowing in an undisturbed environment, and it was shown that the assumption of an undisturbed environment leads to values of the vertical velocity and the vertical acceleration that are vastly in excess of what is believed to occur in the atmosphere.

In the slice method a horizontal slice of air of unit thickness is considered. Let M′ be the mass that moves upwards and M the mass that moves downwards through the slice, and let the corresponding velocities be w′ and w. On the assumption that the slice is so large that the transport of mass through the vertical walls is negligible in comparison with the transport through the horizontal faces, there must be as much transport of mass uppwards as downwards through the slice, or

$$M'w' = -Mw \qquad (13)$$

The theory underlying the slice method has been described in detail elsewhere (Petterssen 1940), but a simplified derivation of the essentials will be given here in order to show more precisely the points where the slice method renders results that differ from those obtained by the parcel method. In particular, we shall be concerned with the relationship between the areas on the TePhi-gram and the vertical velocity and acceleration.

We consider a schematical TePhi-gram as shown in Fig. 3.

Let the line AB represent the ascent curve at the initial moment. We consider the point A on the ascent curve (whose pressure is p_0) and

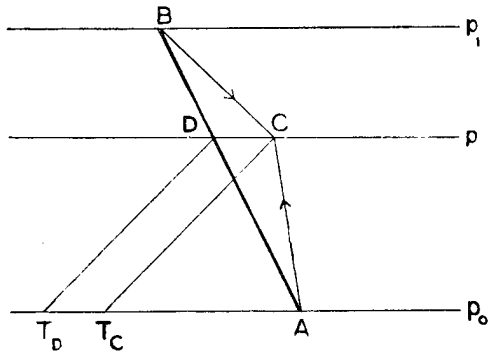

Fig. 3. — Schematical section of a TePhi-gram.
AB = temperature curve;
AC = saturated adiabatic;
BC = dry-adiabatic.

assume that the air at this point is saturated. If this air ascends, it will move along the saturated adiabatic and arrive at the point C on the isobar p. To maintain continuity, a certain mass must descend, and if the descending air is non-saturated (as it would be outside a cloud), it will move along a dry-adiabatic. The following is readily seen from Fig. 3.

(1) The condition for the ascending air to arrive at the isobar p without any excess temperature is that the descending air at the level originated from the level B.

(2) The condition for the ascending air to arrive at the isobar p with a temperature in excess of its environment is that the descending air originated at some level lower than B.

(3) The condition for the ascending air to arrive at the isobar p with a temperature lower than that of its environment is that the descending air originated at some level higher than B.

(4) If the environment remained undisturbed (as is assumed in the parcel method), the excess temperature of the ascending air at C would be

$$\triangle T = T_C - T_D = (\gamma - \gamma_s)\triangle z$$

It will thus be seen that, in the case illustrated in Fig. 3, the parcel method gives an excess temperature of the ascending air that is too high, and, therefore, an acceleration that is too large.

On the above principles, it is easy to obtain a general formula for the excess temperature of the ascending air. Let γ be the lapse rate as shown by the ascent curve in Fig. 3, Γ the adiabatic lapse rate of the descending air, and Γ' the adiabatic lapse rate of the ascending air. (If both masses are either saturated or non-saturated, $\Gamma = \Gamma'$).

The excess temperature of the ascending air after a time interval t is then

$$\begin{aligned}\triangle T &= T' - T = T_A - \Gamma' w't - (T_B - \Gamma wt)\\ &= T_A - T_B + (-\Gamma' w' + \Gamma w)t\\ &= -\gamma (w - w')t + (-\Gamma' w' + \Gamma w)t\end{aligned}$$

and from eq. (13)

$$\triangle T = w't\left[\gamma - \Gamma' - \frac{M'}{M}(\Gamma - \gamma)\right] \qquad (14)$$

or since

$$w't = \triangle z$$

$$\triangle T = \triangle z\left[\gamma - \Gamma' - \frac{M'}{M}(\Gamma - \gamma)\right] \qquad (15)$$

and also from eq. (13)

$$\triangle T = \triangle z\left[\gamma - \Gamma' + \frac{w}{w'}(\Gamma - \gamma)\right] \qquad (16)$$

In the above formulae, w is by definition negative and w′ positive.

The geometrical interpretation of the above equation is readily obtained from Fig. 4. Thus, if the air at A ascends to C, and the air at B descends to E in the time interval t, we have for the excess temperature of the ascending air when it arrives at the isobar p:

$$\begin{aligned}\frac{\triangle T}{(\gamma - \Gamma')w't} &= \frac{EC}{DC} = 1 - \frac{DE}{DC} = 1 - \frac{DF}{DA}\\ &= 1 - \frac{DF}{DB}\cdot\frac{DB}{DA} = 1 - \frac{DG}{DE}\cdot\frac{DB}{DA}\\ &= 1 - \frac{\Gamma - \gamma}{\gamma - \Gamma'}\left(-\frac{w}{w'}\right) = 1 - \frac{\Gamma - \gamma}{\gamma - \Gamma'}\cdot\frac{M}{M'}\end{aligned}$$

or, since $w't = \triangle z$

$$\triangle T = \triangle z\left[\gamma - \Gamma' - \frac{M'}{M}(\Gamma - \gamma)\right]$$

which is identical to eq. (16).

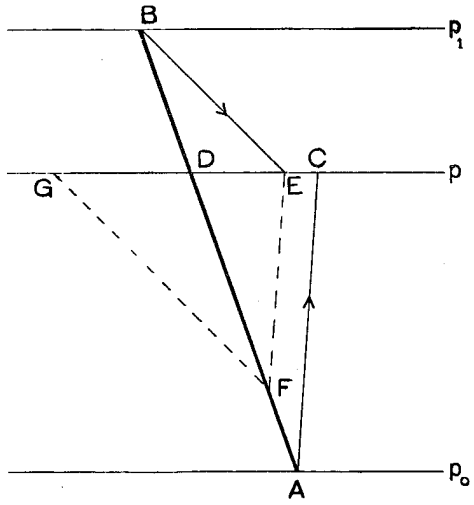

Fig. 4 — Schematical section of a TePhi-gram. AB = temperature curve; AC = adiabatic of the ascending air; BE = adiabatic of the descending air. The excess temperature is proportional to EC. The ascending velocity is proportional to AC, and the descending velocity is proportional to BE.

Eq. (16) can now be specialized as follows:

(1) If both the ascending and the descending masses are non-saturated (e.g. under the cloud base).

$$\Gamma = \Gamma' = \gamma_d$$

and the excess temperature of the ascending air is

$$\triangle T = \triangle z\left(1 + \frac{M'}{M}\right)(\gamma - \gamma_d) = \triangle z\left(1 - \frac{w}{w'}\right)(\gamma - \gamma_d) \qquad (17)$$

In the parcel method w = 0 and therefore

$$\triangle T = \triangle z\,(\gamma - \gamma_d) \qquad (17a)$$

It will thus be seen that the parcel method and the slice method give the same sign of the excess temperature, but the parcel method underestimates the amount of excess temperature in dry convection.

(2) If both the ascending and the descending masses are saturated (e.g. within the cloud)

$$\Gamma - \Gamma' = \gamma_s$$

and the excess temperature of the ascending air is

$$\begin{aligned}\triangle T &= \triangle z\left(1 + \frac{M'}{M}\right)(\gamma - \gamma_s)\\ &= \triangle z\left(1 - \frac{w}{w'}\right)(\gamma - \gamma_s)\end{aligned} \qquad (18)$$

In the parcel method w = 0 and therefore

$$\triangle T = \triangle z\,(\gamma - \gamma_s) \qquad (18a)$$

It will thus be seen that the parcel method and the slice method give the same sign of the excess

temperature, but the parcel method underestimates the amount of excess temperature in saturated convection.

(3) If the ascending air is saturated and the descending air non-saturated (as is the case when we consider a cumulus cloud relative to its environment), the excess temperature of the ascending air is

$$\begin{aligned}\triangle T &= \triangle z\left[\gamma-\gamma_s-\frac{M'}{M}(\gamma_d-\gamma)\right]\\ &= \triangle z\left[\gamma-\gamma_s+\frac{w}{w'}(\gamma_d-\gamma)\right]\end{aligned} \qquad (19)$$

In the parcel method $w = 0$ and, therefore,

$$\triangle T = \triangle z\,(\gamma-\gamma_s) \qquad (19a)$$

It will thus be seen that the parcel method may, or may not, give the right sign of the excess temperature of the ascending air, and the parcel method greatly overestimates the amount of excess temperature.[1])

It will be seen from eq. (19) that the excess temperature vanishes and the stratification becomes neutral when

$$\frac{M'}{M}=\frac{\gamma-\gamma_s}{\gamma_d-\gamma} \qquad (20)$$

or

$$-\frac{w}{w'}=\frac{\gamma-\gamma_s}{\gamma_d-\gamma} \qquad (20a)$$

This shows that, for any given lapse rate, there is an upper limit of the ratio M'/M such that, if this ratio is exceeded, the stratification become stable even when $\gamma > \gamma_s$, in contradiction to the parcel method (i.e. eq. (19a)).

7. The Slice Method: The Positive Area.

It is readily seen from Fig. 4 that the slice method, when applied to cloud producing convective currents, renders positive areas that are much smaller than those indicated by the parcel method. According to the parcel method, the positive area of the parcel that has ascended the small distance from A to C, is represented by the triangle ACD, whereas the positive area according to the slice method, is represented by the triangle ACE. From this it follows that the vertical velocities and accelerations computed by the aid of the parcel method are much too large when saturated air ascends through a dry-adiabatically descending environment. It will also be seen that when the ratios represented by eqs. (20) are exceeded, there will be a negative area according to the slice method, although the parcel method may give a very large positive area.

It is of interest to compare the results of the slice method with those obtained by the parcel method as far as the classification of the ascent curves are concerned. We return to Fig. 2 (para. 3) and note that at the level D

$$\gamma = \gamma_s$$

If convection occurs below the level D, and a rising mass approaches this level, the air at the level D will be given an upward impulse, but according to eq.(19) this air will be stable and resist upward motion. In fact, stability would occur even below the level D, for the air would be stable for all impulses where

$$\frac{M'}{M} > \frac{\gamma-\gamma_s}{\gamma_d-\gamma}$$

Since, in the layer just below D, γ differs only slightly from γ_s, this layer would be stable, except for rising masses which are exceedingly small as compared with the descending masses. Above the level D, the air would be stable for all impulses from rising masses from below, with the result that the part of the positive area above the level D in Fig. 2 does not become available for the rising masses from below.

With regard to the positive area shown in Fig. 2, the above discussion has shown:

(1) *that the positive area below the level D is greatly reduced as a result of the adiabatic heating of the environment,* and

(2) *that the positive area above the level D is fictitious inasmuch as it does not become available for the creation of convective currents.*

There is also a third factor in operation that tends to reduce the positive area of an ascending mass. A certain amount of mixing of heat and moisture will occur between the rising and sinking elements, with the result that the excess temperature and the corresponding positive area are reduced relative to the values indicated by the

[1]) Except, in rare cases, when the lapse rate within the layer containing the convective clouds exceeds the dry-adiabatic lapse rate.

parcel method. The statistical results in Section III seem to indicate that less than 25 per cent of the positive area shown in Fig. 2 actually becomes available for the creation of convective currents.

In view of the results obtained by the aid of the parcel method with regard to the top of the convective clouds and the penetration of the cloud tops into the upper negative area, as discussed in para. 4, it is of interest to examine in greater detail the processes at, and above, the level D in Fig. 2.

We consider a rising mass of saturated air in the layer below D. As this mass imparts an upward impulse to the air at the level D, the lapse rate at the level D may change. It is, therefore, of interest to determine whether the stability of the layer at, and above, D will increase or decrease with time.

In saturated-adiabatic motion the temperature change per unit time at a fixed point is

$$-\frac{\partial T}{\partial t} = w\,(\gamma_s - \gamma)$$

Differentiating with regard to z and noting that

$$-\frac{\partial^2 T}{\partial z\,\partial t} = \frac{\partial \gamma}{\partial t}$$

we obtain

$$\frac{\partial \gamma}{\partial t} = \frac{\partial w}{\partial z}(\gamma_s - \gamma) + w\frac{\partial}{\partial z}(\gamma_s - \gamma) \qquad (21)$$

But at the level D $\gamma = \gamma_s$, and therefore

$$\frac{\partial \gamma}{\partial t} = w\frac{\partial}{\partial z}(\gamma_s - \gamma) \qquad (22)$$

Since $(\gamma_s - \gamma)$ increases from below upwards through the layer D, the lapse rate at D will increase when the saturated ascent reaches the level D, i.e. the stable layer will tend to ascend. However, on account of the stability above the level D, $\frac{\partial w}{\partial z}$ must be negative, and immediately above the level D the first term in eq. (21) comes into play, and its contribution is to reduce the lapse rate. At still higher levels $w = 0$ and the first term in eq. (21) takes control, with the result that there is a tendency for the convective currents to create a stable layer, or an inversion, at some small distance above the layer D. These results are in agreement with those obtained by Rossby (1932).

Thus, each convective current that approaches the level D in Fig. 2, will tend to lift this level slightly, and, at the same time, create increased stability in the layer above D. In Fig. 5 the full curve indicates the initial ascent curve, and the pecked curve the temperature distribution that results from repeated attacks by saturated convection from below.

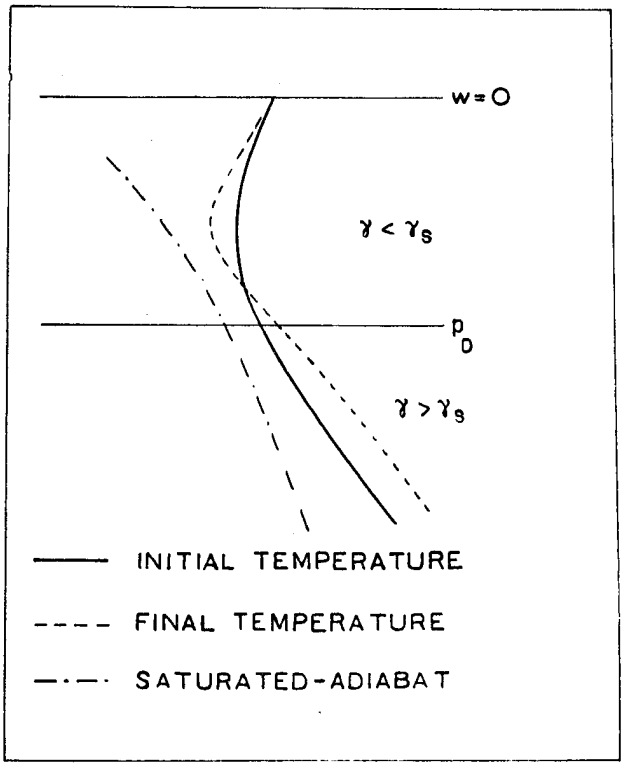

Fig. 5. Schematical section of a TePhi-gram showing the change of stability in the upper part of the convective layer.

8. Further Remarks on the Vertical Velocity.

It was shown in the foregoing paragraphs that the parcel method underestimates the excess temperature and the vertical accelerations and velocities below the cloud base and also within the cloud, whilst it greatly exaggerates the excess temperature and the vertical accelerations and velocities of the cloud air relative to the environment.

Experience shows that the convective cloud is not a uniformly ascending mass but a complex system of irregular currents. Although the mean velocity through a horizontal section of the cloud is upward, there are a number of downward currents alternating with upward gusts of considerable intensity. The life of each of the upward and

downward moving elements within the cloud is short as compared with that of the cloud as a whole. Distinction must therefore be made between the general upward current of the cloud and the superimposed gusts.

The strength of the general upward current can be assessed roughly in two different ways.

1. Consider a cloud that has just formed. Even in pronounced cases it is rarely observed that the top of the growing cumulus rises more rapidly than 2 Km per hour, or 0.6 m/sec, even when a large positive area is present. As will be shown in Section III, a velocity 0.6 m/sec is only about 6 per cent of the velocity that would be obtained by the parcel method, showing that the vertical velocities obtained by the parcel method for saturated ascent through a dry-adiabatically descending environment are much too large.

2. Let I be the mean rain intensity per unit area under the cloud, a the mean absolute humidity below the cloud base, and let w be the mean upward velocity through the cloud base. When the steady state is reached, i.e. when the cloud neither grows nor accumulates water

$$I = a\,w$$

If the rain intensity is 36 mm per hour, and a is 15 gm/m^3

$$w = 0.7 \text{ m/sec}$$

which agrees with the value indicated above.

Since the above rain intensity is very large as a mean value under a whole cloud while the indicated absolute humidity is not excessive, it is reasonable to assume that the mean velocity of the cloud mass is not likely to exceed about 0.7 m/sec. To create such velocities, only a small difference between the virtual temperature of the cloud and the surrounding air is required.

With regard to the gusts that are often observed below the cloud base, and also within the cloud, different considerations hold, for the parcel method underestimates the amount of available energy when both the ascending and descending currents follow the same adiabatic.

Under the cloud base the lapse rate is normally only slightly super-adiabatic, with the result that the positive area below the cloud base is very small and the vertical gusts not excessive.

However, when the ascending air, with a slightly super-adiabatic lapse rate, reaches the condensation level, a relatively large positive area is immediately available, and the large accelerations occur. On the other hand, the volumes of the rising bubbles are small as compared with that of the cloud, and turbulent mixing will rapidly reduce the excess temperature of the individual bubbles, with the result that the life of each bubble is relatively short. The strength of the vertical gusts within the cloud will depend not only upon the lapse rate within the cloud but also upon the life of the individual bubbles. The observations discussed in Section III are not sufficiently detailed for a reliable assessment of the strength of the vertical gusts within the cloud, but some statistics are given with regard to the maximum lapse rates that have been observed within convective clouds.

9. The Slice Method: Cloud Base, Top and Amount.

1. *The condensation level.* The method of evaluation of the condensation level is independent of the assumptions underlying the parcel method and the slice method, and the discussion in para. 4 applies to both. The evaluated condensation levels have been compared with the observed base and the results are given in Section III.

2. *The top of convective clouds.* According to the parcel method, the top of the convective cloud should be found at, or near, the top of the upper negative area, i.e. at the level GF in Fig. 2. According to the slice method, the stable layer commences already at the level D, and energy consumption commences already below the level D. Although the ascending currents may penetrate some distance into the stable layer, it follows from the discussion in para. 7 that the distance above the level D, to which the cloud tops can reach, must be relatively small. According to the slice method, therefore, the top of the convective cloud will be found at some small distance above the level D, i.e. the level at which the actual lapse rate equals the saturated-adiabatic rate. In this connection it is of interest to note that when an inversion is present, and the positive area below the inversion is small, the top of the upper negative area and the top of the positive area will not be very far above the level D. In

these circumstances the slice method and the parcel method will render results that do not differ greatly. As will be shown in Section III, very large differences are found when the stability above the level D is slight.

3. *Cloud amounts.* It was shown in para. 6 that, for any given lapse rate, there is a value of the ratio of the ascending mass to the descending mass which, when exeeded, causes the stratification to become stable, even when the lapse rate exceeds the adiabatic rate. This ratio is expressed by eq. (20). Since M′ and M denote the masses contained within a slice of unit thickness, the ratio of the masses may be replaced by the ratio of the areas involved. Accordingly, the limit at which energy production ceases is expressed by

$$\frac{A'}{A} = \frac{\gamma - \gamma_s}{\gamma_d - \gamma}$$

where A′ is the horizontal area through which the air ascends, and A is the horizontal area through which the air descends. This ratio applies to the energy-producing clouds, i.e. the clouds that have a temperature in excess of that of the environment. In addition to the energy-producing clouds, passive, or energy-consuming clouds may be present. However, if convection is active, the energy-consuming and the passive clouds cannot exist in appreciable amounts, for these clouds will dissolve in the descending currents. As a result of this, the amount of clouds in active convection is not likely to exceed much the amount indicated by the above ratio.

In this connection it is of interest to note that the cloud amount assessed by the ground observer represents a projection of the cloudy areas on the sky. These cloud amounts are, therefore, exaggerated on account of the perspective effect. The air observer, on the other hand, will report cloud amounts representing more nearly the true ratio of the cloudy and the clear spaces. Thus, the amounts reported by the air observer are largely comparable with the ratio referred to above.

In typical situations the lapse rate in the convective cloud layer is rarely greater than

$$\tfrac{1}{2}(\gamma_d + \gamma_s)$$

with the result that the ratio of the cloudy to the clear area is not likely to exceed unity, and the observed cloud amounts (assessed without the perspective effect) are not likely to exceed five-tenths. This holds for active convection (i.e. energy-producing clouds). When an inversion is present, the convective clouds spread out under it in the energy-consuming layer. The typical cloud form is then strato-cumulus, or a layer of flat cumulus, and the amount of these clouds often exceeds five-tenths of the sky. A comparison between the above theoretical results and observed cloud amounts is given in para. 18.

10. The Convection Temperature.

We consider a stable layer of air above the ground as shown in Fig. 6. If the air at A were lifted adiabatically and with constant moisture content, it would become saturated at its condensation level C. If the air at A is heated with constant moisture content, the level C will rise, and by the time the surface temperature has reached the value T_c, the condensation level will have ascended to the point B on the ascent curve. If, at this time, a dry-adiabatic lapse rate has been established below the level B, convection from the ground would be released and the ascending air would reach the condensation level B. The temperature indicated by T_c in Fig. 6 is called the *convection temperature*; its evaluation from the TePhi-gram is evident from Fig. 6.

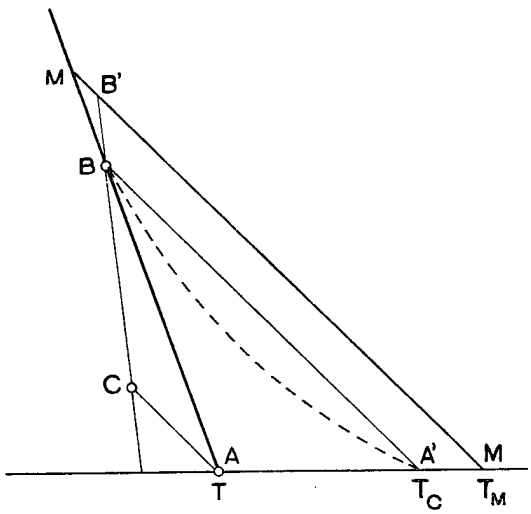

Fig. 6. Schematical section of a TePhi-gram. AB = temperature curve at sunrise; CB = line of constant humidity mixing ratio; AC, A′B and MM = dry-adiabatic; T_C = convection temperature; T_M = maximum temperature.

The area ABA′ in Fig. 6 indicates the amount of heat that must be supplied per column of unit cross section of the layer below the level B in order to establish a dry-adiabatic lapse rate down to the ground.

The above deduction rests on the assumption that the moisture content of the air remains constant during the process. Normally, the heating of the ground would intensify evaporation, and the humidity mixing ratio would increase, with the result that the condensation level B would be found at some lower level, and the convection temperature corresponding thereto would be less than that indicated in Fig. 6. Furthermore, if a slightly super-adiabatic lapse rate is maintained above the ground (as indicated by the pecked curve in Fig. 6), less supply of heat to the layer would be needed to release convection.

However, as long as the humidity mixing ratio remains unchanged, the temperature T_c must be reached before the negative area below B is eliminated. It will thus be seen that the area ABA′ represents the maximum amount of energy that must be supplied prior to the appearance of convective clouds. A super-adiabatic lapse rate above the ground will substantially reduce this area, but the temperature T_c would not be affected as long as the humidity mixing ratio does not change.

In the early morning there is often a minimum of moisture near the ground. In such cases a representative value of the humidity mixing ratio must be used. It has been customary to assume that the humidity mixing ratio will mix and become uniform along the vertical by the time convection commences, with the result that the mean humidity of the layer rather than the observed values at the ground should be used for assessing the convection temperature.

The convection temperature is of considerable use in the forecasting of convection due to diurnal heating, and the success that can be obtained depends largely upon the ability of the forecaster to estimate whether or not the actual midday temperature will reach (or exceed) the critical value. In this assessment the forecaster will be guided not so much by the difference T_c—T in Fig. 6 as by the size of the area ABA′, for if the lapse rate is steep, the heating will be spread over a deep layer, and the diurnal amplitude of temperature will be small.

An assessment of the amounts of heat supplied to the surface layer through diurnal insolation has been made by Gold (1933), who converted the amounts of heat into areas on the Te-Phi-gram. This conversion is not exact, but it is sufficiently accurate in comparison with the errors introduced by the observational material and the assumptions underlying the derivation. The values obtained by Gold are given in Table D. As regards the method of derivation, etc., the reader is referred to the original paper.

The areas in Table D represent the amounts of energy supplied during the period from sunrise until the maximum temperature is reached. This area is represented by AMM in Fig. 6, where T_M indicates the diurnal maximum temperature. It will be seen that if the lapse rate above the ground is super-adiabatic, a substantially smaller area will give the same maximum temperature. In this connection it may be mentioned that Swinbank (1944), on the basis of more plausible assumptions as to the exchange of heat between the air and the ground, finds amounts of energy which are smaller than those given in Table D. However, when the energy values found by Gold and Swinbank are converted into maximum temperature, the results are in good agreement.

Table D.

Monthly Values of Available Heat from Sunrise to early Afternoon and the corresponding Areas on the TePhi-gram (according to Gold).

Month	gm. cal/cm²	Area (cm²)
January	40	1.8
February	70	3.1
March	100	4.4
April	140	6.2
May	175	7.8
June	180	8.0
July	165	7.3
August	150	6.7
September	115	5.1
October	80	3.6
November	40	1.8
December	30	1.3

The areas indicated in Table D have been applied in connection with the analysis of a num-

ber of TePhi-grams in situations where the convection was due to diurnal heating, and a comparison between the computed and the observed results is given in para. 22.

11. The Use of Virtual Temperature.

In the foregoing paragraphs we have discussed convection in terms of air temperature, i.e. as if the influence of the moisture content on the density of the air was accounted for in the gas constant. Since the TePhi-gram, and other similar diagrams, are constructed on the basis of the gas constant for dry air, it is necessary, when applying the theoretical results to TePhi-grams, to introduce the virtual temperature to account for the density difference between the ascending and the descending masses. Thus, the results derived in the foregoing paragraphs are applicable to the TePhi-grams, when *virtual temperature replaces the dry-bulb temperature, and the virtual saturated-adiabatics replace the ordinary saturated-adiabatics.*

1. *The virtual temperature.* The total density of the moist air is the sum of the density of the dry air and of the aqueous vapour. If ϱ is the density of the moist air, p the atmospheric pressure, and e the vapour pressure

$$\varrho = \frac{p - e}{RT} + 0.622\,\frac{e}{RT} = \frac{p}{RT}\left(1 - 0.378\frac{e}{p}\right)$$

where R is the gas constant of dry air, and T the absolute temperature. The virtual temperature T_v is then defined as the temperature that the dry air would have if its density were ϱ and its pressure p. Hence

$$T_v = \frac{T}{1 - 0.378\,\frac{e}{p}}$$

Now, the humidity mixing ratio is

$$q = \frac{0.622\,e}{p - e}$$

Since q is of the order of 10^{-2}, second and higher powers of q may be neglected. With sufficient accuracy therefore

$$T_v = T\,(1 + 0.6\,q)$$

where T_v and T are expressed in °A.

When the air temperature is below 0°F (i.e. about — 18°C) the humidity mixing ratio is so small that the virtual temperature increment falls below the observational accuracy. At these low temperatures, therefore, the virtual temperature increment may be neglected. At high temperatures, however, the virtual temperature increment becomes important. For example, at 90°F and 1000 mb the virtual temperature increment may be as large as 10°F. If the air outside the cloud is relatively dry, large density contrasts may exist on account of the difference in the humidity inside and outside the cloud. In such cases *the cloud air may be lighter than the environment although the air within the cloud may be colder than the surrounding air.*

2. *The virtual saturated-adiabatics.* We consider a schematical TePhi-gram as shown in Fig. 7. A parcel of air has the temperature T, the wet-bulb temperature T_w, and the virtual temperature T_v. If this parcel ascends, T and

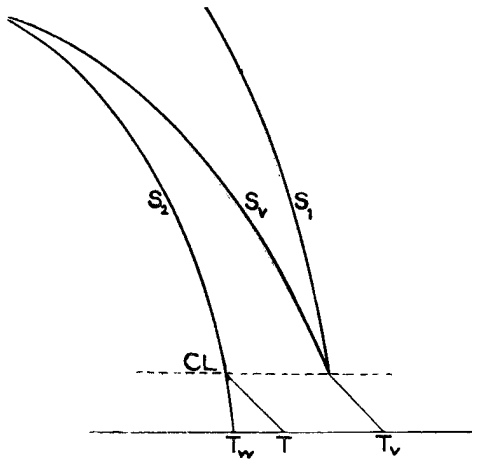

Fig. 7. — Schematical section of a TePhi-gram. As the air ascends above the condensation level CL, the virtual temperature decreases at a rate faster than the saturated adiabatic S_1. Hence, the virtual saturated-adiabatic lapse rate is steeper than the ordinary saturated-adiabatic rate.

T_v will vary dry-adiabatically until the condensation level CL is reached. It will be seen that the condensation level is evaluated from the dry-bulb and the wet-bulb temperatures, and not from the virtual temperature.

As the parcel ascends above the condensation level, the temperature point will follow the saturated-adiabatic S_2, but the virtual temperature will *not* follow the saturated-adiabatic S_1, for, as water is condensed, the virtual temperature increment will decrease and approach zero at temperatures below about 0°F. Hence, the virtual temperature of the ascending saturated air will

decrease as indicated by the curve S_v in Fig. 7, i.e. the *virtual saturated-adiabatic.*

In the analysis of the TePhi-grams described in Section III the virtual temperature and the virtual saturated-adiabatics have been used.

12. Remarks on the Observational Accuracy.

For the evaluation of such quantities as the condensation level, the convection temperature and the positive and the negative areas, the surface observations are used, and the errors in these observations will influence the accuracy of the evaluated quantities. The following is readily obtained from a TePhi-gram.

To an error of $\pm$ 1°F in the surface dry-bulb temperature corresponds: (1) an error $\pm$ 1°F in the virtual temperature, (2) no error in the convection temperature, and (3) an error of $\mp$ 10 to 15 mb in the condensation level. In convective situations the negative area is either very small or absent. An error of $\pm$ 1°F in the surface dry-bulb temperature will then have no appreciable influence on the accuracy of the evaluated positive area, and the error in the negative area is proportional to the distance to the condensation level.

To an error of $\pm$ 1°F in the surface wet-bulb temperature corresponds: (1) No appreciable error in the virtual temperature, (2) a $\mp$ error in the convection temperature, the magnitude of which varies greatly with the lapse rate, (3) an error of $\pm$ 10 to 15 mb in the condensation level, (4) a $\mp$ error in the negative area, the magnitude of which varies with the shape of the ascent curve, and (5) a $\pm$ error in the positive area, the magnitude of which is proportional to the length of the positive area.

It is readily seen (e.g. from Fig. 2) that as far as the positive area is concerned, an error of $\pm$ 1°F in the surface wet-bulb temperature has the same effect as an error of $\pm$1°F in the dry-bulb temperature throughout the air column. It will thus be seen that a high degree of accuracy is required in the surface humidity observations.

13. Release of Precipitation.

According to Bergeron (1933), the presence of ice crystals and super-cooled water droplets in the clouds is an essential condition for colloidal instability. The instability is due to the depression of the saturation vapour pressure over ice, which has a maximum at about 10°F. When the temperature in the upper part of the cloud is appreciable below freezing, the cloud would become colloidably unstable and precipitation would be released.

Computations show (Houghton 1939, Petterssen 1941) that the growth of the cloud droplets through condensation decreases rapidly when the drops increase, and the colloidal instability due to ice crystals can only account for the initial growth from ice crystals to large cloud elements, but is insufficient to account for the size of the raindrops. However, as the larger cloud elements will fall more rapidly than the smaller elements, coalescence through collisions will occur, and the falling drops will increase in proportion to the depth of the cloud through which they fall.

A number of ascents made in convective situations with precipitation has been analyzed and classified according to the temperature in, and the depth of, the clouds. The results are given in Section III.

III. STATISTICAL CHARACTERISTICS

As far as the observational material has been found suitable, the theoretical results referred to in the foregoing section have been tested against the analysis of synoptic charts and the observations of temperature, humidity, etc., in the free atmosphere. The results of this comparison are summarized in the following paragraphs.

14. The Observational Material.

The temperature and humidity soundings chosen for the statistical treatment refer to Bircham Newton and Aldergrove. The observations are made in aircraft ascending spirally to the 400 mb surface. Simultaneous observations of temperature, humidity and pressure are made at intervals of 50 mb and also at significant points. The cloud forms, their bases, tops and amounts are noted by the observer in the aircraft. The cloud observations reported at the synoptic hours by the ground stations have also been used.

The radio-sonde observations of temperature and humidity made at various stations in the

British Isles have not been used, since these soundings are not supplemented by cloud observations from the free atmosphere.

Certain aspects of convection have been correlated with the wind observations in the free atmosphere. For this purpose the radio-wind soundings from Downham Market have been used and correlated with the simultaneous temperature soundings from Bircham Newton. These two stations are sufficiently near one another for the two sets of observations to be comparable.

The occurrence of shallow and deep convection has been correlated with the shear and the curvature of the flow in the 750 mb surface, the shear and curvature being obtained from the contours of the said pressure surface.

The principal aim of the statistical investigation has been to determine the applicability to upper air soundings of the theoretical relationships set out in Section II. Inasmuch as the criteria for stability and instability may be capable of accounting for the occurrence of convective phenoma without being capable of rendering satisfactory numerical results, it is necessary to test the mere occurrence as distinct from the numerical fit.

For the occurrence test it is necessary to treat a continuous series of observations chosen at random, which contains a sufficient number of convective as well as non-convective cases. For this purpose the soundings from Bircham Newton for the period June—August, 1943, have been analysed. This series comprises 276 individual soundings, during 142 of which the air observer reported the presence of convective clouds. This series of observations will be referred to as the *non-selected series.*

For the test of the numerical accuracy of the various criteria and theoretical relationships the soundings from Bircham Newton and Aldergrove for the period April—November, 1943, have been used, and 295 cases of convection were chosen for investigation. The selection of convective situations was made by inspection of the sea level synoptic charts, and a situation was selected for investigation, if it was found to satisfy the following conditions:

(1) convective clouds with or without precipitation reported at or near Bircham Newton or Aldergrove.

(2) no front present within 200 miles of these stations.

This selection aims at the exclusion of convection released by fronts, i. e. convection that does not necessarily commence at the ground. A detailed analysis of the individual soundings showed that a few of the selected cases represented convection due to fronts which were so feeble that they had not been introduced in the surface analysis. These cases will be discussed separately.

It is of interest to note that the soundings themselves were not used for selecting the convective situations, nor was any attempt made at selecting according to intensity of convection, type of synoptic situation, etc. The statistical results should therefore represent a fair cross-section of the conditions typical for convection within the British Isles. Finally, it may be noted that mid-winter situations were excluded on account of the reduced quality of the cloud observations at the times of the morning and evening ascents.

15. Characteristics of the Selected Situations.

Certain statistical characteristics of the selected synoptic situations at sea level are given in Tables I—V.

Table I.

Percentage Frequency of Wind Directions at Station Level.

	Aldergrove	Bircham Newton	Mean
NE	0.6	1.6	1.1
E	1.8	0.8	1.3
SE	3.6	0.8	2.2
S	4.8	2.3	3.5
SW	13.2	14.7	14.0
W	30.2	30.2	30.2
NW	32.0	27.1	29.5
N	9.0	21.7	15.4
Calm	4.8	0.8	2.8

Table II.

Percentage Frequency of Wind Force at Station Level.

Force	Aldergrove	Bircham Newton	Mean
0	4.8	0.8	2.8
1	5.4	3.9	4.6
2	22.9	7.8	15.4
3	29.6	24.0	26.8
4	26.5	34.1	30.3

Table II, cont.

Force	Aldergrove	Bircham Newton	Mean
5	9.6	21.7	15.6
6	1.2	5.4	3.3
7	—	2.3	1.2

Table III.

Percentage Frequency of M.S.L. Pressure.

Pressure (mb)	Aldergrove	Bircham Newton	Mean
980—89	1.8	1.5	1.7
990—99	13.2	5.4	9.3
1000—09	23.5	26.4	25.0
1010—19	40.4	41.1	40.7
1020—29	17.5	23.3	20.4
1030—39	3.6	2.3	2.9

Table IV.

Precentage Frequency of Barometric Tendencies.

Tendency (mb)	Aldergrove	Bircham Newton	Mean
$\geqslant$ 3.0	7.8	3.2	5.5
2.0 to 2.9	4.2	10.0	7.1
1.0 to 1.9	24.7	17.8	21.3
0.0 to 0.9	32.1	32.5	32.3
— 0.1 to — 1.0	19.8	27.8	23.8
— 1.1 to — 2.0	9.6	4.7	7.1
— 2.1 to — 3.0	1.8	1.6	1.7
$<$ — 3.0	—	2.4	1.2
Mean Tendency	0.6	0.5	0.6

Table V.

Percentage Frequency of Curvature of M.S.L. Isobars.

Curvature	Aldergrove	Bircham Newton	Mean
Cyclonic	36	42	39
Straight	33	37	35
Anticyclonic	31	21	26

It will be seen from Table I that about 75 per cent of the selected cases occurred with surface wind directions from W, NW or N, suggesting a preponderance of polar outbreaks. The relatively high wind forces shown in Table II suggest that advection rather than diurnal heating is, in the majority of cases, responsible for the creation of instability, although diurnal heating contributes to the creation of steep lapse rates. The times to which the selected ascents refer are shown in Table VI.

Table VI.

Time of Observation	Percentage Frequency of Ascents
Morning	20
Midday	45
Evening	35

It will be seen from Table VI that at least 60 per cent of the selected cases represent convection due to advective heating. The remaining 40 per cent will be due to either pure diurnal heating or diurnal heating assisted by advection.

It will be seen from Table IV that about two-thirds of the selected cases occurred together with rising pressure, and this together with Table I suggests that the majority of the selected cases belong to the rears of travelling depressions, or polar currents spreading eastward. Table V indicates that, on the whole, there is a slight preference for cyclonically curved isobars.

It is important to bear in mind that the characteristics shown in the above Tables do not result from the method of selection of cases, for the cases were selected on the criteria mentioned in para. 14, without regard to the synoptic situation, type of circulation, etc. The above characteristics may, therefore, be taken to indicate the conditions that normally are favourable for the development of convective phenomena over the British Isles.

16. Remarks on Cloud Observations.

The cloud forms and weather phenomena which are generally recognized to result from convective current are:

Cumulus humilis (Cu)
Cumulus congestus (CuC)
Cumulo-nimbus (Cb)
Showers, squalls, thunderstorms and hail.

In many cases it has been found that convection results in strato-cumulus (Sc), particularly when the convective layer is limited upward by a stable layer, or an inversion. Thus, strato-cumulus together with cumulus will often be

found to occur. Quite frequently the convective clouds may appear as well-defined cumuli as seen from the ground, but as a layer of strato-cumulus as seen from the aircraft. This is particularly true when the tops of the individual cumuli appear at an uniform level. In these cases, the ground observer and the air observer may report different types of clouds.

While the ground observer makes distinction between cumulus humilis (i.e. flat cumulus) and cumulus congestus (i.e. towering cumulus), no such distinction is made by the air observer who reports the height of the base and of the top of the cumuli. In the following, no distinction will be made between cumulus humilis and cumulus congestus, both being denoted by the symbol Cu.

The distinction between cumulus congestus and cumulo-nimbus is also difficult, for the tops of these clouds cannot always be seen by the ground observer who, in his assessment, is guided by the appearance of the sky as a whole rather than by the structure of the individual clouds.

A comparison has been made between the cloud forms reported by the ground observers and the air observers in the 295 cases selected for investigation, and the results are shown in Table VII.

Table VII.

Percentage Frequency of Cloud Forms reported by the Ground Observer and the Air Observer. Selected Series.

Air Observer	Ground Observer				Total
	Cb	Cu	Cu & Sc	Sc	
Cb	18	4	1	—	23
Cu	6	20	7	2	35
Cu & Sc	2	9	8	2	21
Sc	1	8	6	6	21
Total	27	41	22	10	100

It will be seen from Table VII that complete agreement between the two observers is obtained only in 52 per cent of the cases. However, an examination of the individual cases shows that the discrepancies represent borderline cases in which it has been difficult to distinguish between flat cumulus and strato-cumulus, or between towering cumulus and cumulo-nimbus, or between cumulus with and without strato-cumulus. Except in three cases (i.e. 1 per cent) where the air observer reported Sc while the ground observer reported Cb, the cloud reports by both observers have been found satisfactory.

In 6 per cent of the cases both the air observer and the ground observer reported Sc without cumulus or other instability phenomena. In these cases it was found that neighbouring stations and the synoptic charts indicated a convective situation. These cases have therefore been included; they may be taken to represent convection within a shallow layer.

17. Occurrence of Convective Clouds.

In order to determine the extent to which the parcel method and Normand's classification of ascent curves (as referred to in para 3.) are capable of accounting for the occurrence of convective clouds, the non-selected series of observations referred to in para. 14 has been used, and the results of the analysis of the ascent curves have been compared with the cloud observations made from the aircraft. In the analysis the negative and the positive areas were evaluated by the use of virtual temperatures and the virtual saturated-adiabatics, as explained in para. 11.

The non-selected series covers the period June —August 1943. It refers to Bircham Newton and contains 270 ascents with cloud observations.

If, following Normand, the criterion for instability is that the positive area is greater than the negative area, and, similarly, the criterion for stability is that the negative area is greater than the positive area, the 270 ascents with cloud observations can then be referred to four categories, viz.,

A. The positive area greater than the negative area with clouds of the cumulus type.[1])
B. The positive area smaller than the negative area without clouds of the cumulus type.
C. The positive area greater than the negative area without clouds of the cumulus type.
D. The positive area smaller than the negative area with clouds of the cumulus type.

[1]) By clouds of cumulus type is here understood Cu and Cb, and not Sc.

The percentage frequency of the above categories were found to be as shown in Table VIII.

Table VIII.

Category	Percentage Frequency
A	43
B	25
C	21
D	11
A + B	68
C + D	32

It will be seen from Table VIII that the cloud observations confirmed the criterion for instability in 43 per cent of the cases (i.e. category A), and confirmed the criterion for stability in 25 per cent of the cases. Thus, in all, the criteria gave satisfactory results in 68 per cent of all cases. The frequencies in the categories C and D represent the number of cases in which the cloud observations failed to confirm the criteria.

The failure of the criteria to render the expected results is not symmetrical, for the frequency in category C is about twice as large as that in category D, i.e. there is a small number of cases with cumulus clouds in contradiction to the criterion for stability, but a fairly large number of cases where the criterion for instability was satisfied without clouds of the recognized convective type resulting.

Category B is of no further interest, for neither the criteria nor the observations indicate that any form of instability was present.

Category C is of considerable interest; the criteria indicate that instability is present, but the observations show no cloud of the recognized convective type (i.e. Cu or Cb).

Of the 58 observations in category C, 48 showed strato-cumulus and 6 stratus; in 4 cases no low clouds were observed.

We shall first consider the four cases in which the instability criterion was satisfied without low cloud being present. In three of these cases there was no negative area at all, i.e. super-adiabatic lapse rate above the ground. However, the air was so dry that the condensation level was well above the top of the positive area, with the result that no cloud could form. In the fourth case the positive area was slightly larger than the negative area, but there was a strong inversion at the ground which, apparently, prevented convection from being released. The ascent referred to was made on 24th August, 1943, at 0600 G.M.T. At 1200 G.M.T. the diurnal heating had eliminated the negative area, and cumulus cloud had formed. Thus, on closer examination, the lapse rate criteria of the parcel method and of the slice method (see paras. 1 and 6) were fully satisfied.

We shall next examine the 54 cases in which strato-cumulus (48) and stratus (6) were reported in category C. The frequency of occurrence of these clouds in relation to the negative and positive areas is shown in Table IX.

Table IX.

Frequency of Strato-cumulus and Stratus in Combinations of Positive and Negative Areas. Non-selected Series, Category C. (Figures in Parentheses refer to Stratus).

Positive area (cm^2)	Negative Area (cm^2)				Total
	0.0	0.1/0.2	0.3/0.4	0.5/0.6	
0.0	—				—
0.1—0.5	13 (2)	1	1		15 (2)
0.6—1.0	12 (1)		1	2	15 (1)
1.1—2.0	8			(1)	8 (1)
2.1—3.0	— (1)				— (1)
3.1—4.0	3				3
4.1—5	—				—
6—10	3 (1)				3 (1)
11—20	1				2
> 20	1	1		1	2
Total	41 (5)	2	2	3 (1)	48 (6)

It will be seen from Table IX that 41 of the 48 cases of strato-cumulus and 5 of the 6 cases of stratus occurred without a negative area being present. In these cases, the lapse rate near the ground was dry-adiabatic or steeper, and there can be little doubt that the clouds were formed through convection. In the remaining cases (i.e. 8 out of 54) the negative area was so slight that, unless the temperature was extremely uniform horizontally, the negative area would be certain to disappear locally. Furthermore, even minor inaccuracies in the observations would give negative areas of the magnitude indicated in Table IX.

It is of interest to note that the positive areas in Table IX are relatively small, and this

suggests that the unstable layers were relatively shallow, i. e. they were limited by stable layers, or inversions, at some distance above the ground.

From the above discussion it appears that the 54 cases represent convective strato-cumulus of the type referred to in para. 9. Thus, recognising this type of strato-cumulus as a convective cloud, it will be seen that the instability criteria of the parcel method and the slice method, as applied to the conditions between the earth's surface and the cloud base, account for the presence, or absence, of convective clouds in 89 % of the cases referred to in Table VIII, i.e. the sum of the frequencies in the categories A, B and C.

Category D. We shall next discuss the clouds in category D in greater detail and compare their characteristics with those of the clouds in category A. The clouds in these categories have been grouped according to the size of the positive and negative areas, and the results are shown in Table X.

Table X.

Frequency of Clouds of the Cumulus Type in Combinations of Positive and Negative Areas. Non-selected Series. Categories A and D.

Positive area (cm²)	Negative area (cm²)												Total	
	0	0.1/0.2	0.3/0.4	0.5/0.6	0.7/1.0	1.1/2.0	2.1/3.0	3.1/5.5	6/10	11/20	21/30	> 30	A	D
0			–	–	–	–	–	–	1	4	1	8	0	14
0.1/0.2	5			–	1	–	2	–	1	–	1	2	5	7
0.3/0.4	3	1			–	1	1	–	–	1	–	–	4	3
0.5/0.6	4	–	–			1	1	1	–	1	–	–	4	4
0.7/1.0	5	2	3	2			–	–	–	–	–	1	12	1
1.1/2.0	12	2	3	–	2			–	–	–	–	–	19	–
2.1/3.0	11	2	–	–	–	–			–	–	–	–	13	–
3.1/5	11	1	1	–	2	–	–			–	–	–	15	–
6/10	13	3	2	1	–	–	–			–	–	–	19	–
11/20	13	–	2	–	3	1	–	–			–	–	19	–
21/30	4	–	–	–	–	–	–	–	–			–	4	–
> 30	5	–	1	–	–	–	–	–	–	–			6	
Total A	86	11	12	3	7	1	–	–	–	–	–	–	120	–
Total D	–	–	–	–	1	2	4	1	2	6	2	11	–	29

Note: The upper right half of the table refers to Category D, and the lower left to Category A.

It will be seen that the clouds of the category A are characterized by the absence of, or a very small, negative area and, on the whole, a very large positive area, which is in agreement with what one would expect. On the other hand, the clouds in category D are characterized by a very large negative area and a relatively small positive area. It is indeed difficult to see how convection could be released from the ground in the numerous cases where there is no positive area but a very large negative area.

In order to throw further light on this question we shall examine the amount and the depth of the clouds in categories A and D. If N denotes the number of tenths of the sky covered by cumulus cloud, and $\triangle p$ the pressure difference between the base and the top of the cloud, we shall define the *equivalent cloud amount* E by

$$E = \frac{N \triangle p}{50}$$

The figure 50 in this formula is introduced as a convenient unit for measuring the depth of the cloud. In the above formula N is the cloud cover as reported by the air observer which, unlike the cloud cover reported by the ground observer, is largely free from the perspective effect. The equivalent cloud amount is readily interpreted. Thus, $E = 2$ means that if the clouds were arranged in a column 50 mb deep, two tenths of the sky would be covered, and similarly, if $E = 20$, there would be sufficient cloud to fill

a 100 mb layer with complete overcast, or a 200 mb layer with half overcast.

The equivalent amounts of cumulus clouds belonging to the categories A and D have been correlated with the difference △A between the positive and negative areas as shown in Table XI, where △A > 0 indicates that the positive area is greater than the negative area (i.e. category A), and △A < 0 indicates that the negative area is greater than the positive area (i.e. category D).

Table XI.

Frequency of Equivalent Amounts of Cumulus Cloud for Various Values of the Difference between Positive and Negative Areas. Non-selected Series. Categories A and D.

△A (cm²)	Equivalent Cloud Amount										Total
	0.2	0.4	0.6	0.8	1.0	1.1/2.0	2.1/5.0	5.1/10.0	10.1/20.0	20	
> 30	–	–	–	–	–	1	1	1	–	3	6
21/30	–	–	–	–	–	–	1	2	1	–	4
11/20	–	–	–	–	1	–	2	2	4	6	15
6/10	–	–	2	–	1	–	1	6	4	4	18
3.1/5	–	–	–	1	1	7	2	–	–	1	12
2.1/3.0	1	2	1	–	–	2	3	4	–	–	13
1.1/2.0	–	1	–	1	–	2	5	3	–	1	13
0.7/1.0	2	–	2	–	–	1	3	–	–	–	8
0.5/0.6	1	–	2	–	–	2	1	–	–	–	6
0.3/0.4	1	–	–	–	–	1	3	–	–	–	5
0.1/0.2	1	–	–	–	3	–	2	–	–	–	6
0	–	–	–	–	–	–	–	–	–	–	–
— 0.1/— 0.2	–	–	–	–	–	–	–	–	–	–	–
— 0.3/— 0.4	–	–	–	–	–	–	–	–	–	–	–
— 0.5/— 0.6	1	–	–	–	–	–	–	–	–	–	1
— 0.7/— 1.0	–	1	–	–	–	–	1	–	–	–	2
— 1.1/— 2.0	1	1	–	–	1	–	–	–	–	–	3
— 2.0/— 3.0	–	–	1	–	–	–	–	–	–	1	2
— 3.1/— 5	–	–	–	–	–	1	–	–	–	–	1
— 6/— 10	–	1	–	–	–	–	–	–	–	–	1
— 11/— 20	2	1	–	–	–	1	–	1	–	–	5
— 21/— 30	–	–	–	–	–	1	–	2	–	–	3
< — 30	2	2	1	1	–	2	–	2	–	–	10
Total A	6	3	7	2	6	16	24	18	9	15	106
Total D	6	6	2	1	1	5	1	5	–	1	28

The upper half of table refers to Category A and the lower half to Category D. This table contains 15 cases less than does Table X, the difference being due to missing observations of cloud top or cloud base.

It will be seen from Table XI that there is some positive correlation between △A and the equivalent cloud amount in category A, but no such correlation in category D. It will also be seen that the majority of the cases in category D represent insignificant equivalent amounts. Only in 7 of the recorded cases in category D are the equivalent amounts appreciable, and all these cases occurred with excessive stability near the ground. Although the possibility of erroneous cloud reports cannot be excluded, the number of such reports is not likely to account for the cases in category D, which represent 11 % of all cases examined. An examination of the synoptic charts showed that most of the cases with high equivalent cloud amounts in category D were associated with fronts, and in these cases convection is not released from the ground, which explains the occurrence of heavy convective clouds although the negative area of the surface air was very large.

A further source of the cases in category D

may be sought in the circumstance that in many cases, notably with small equivalent amounts, convection occurred at sea without the ascent at Bircham Newton showing instability in the surface layer. In this connection it is significant that of the 28 ascents in category D, 17 were made at about 0600, 2 at about 1200, and 9 at 1800 GMT.

Summary: From the above discussion it follows that, with the exception of a few doubtful cases, the criteria of the parcel method and of the slice method for convection to be released from the ground have proved to yield results that are entirely satisfactory. Thus, the criteria are capable of accounting for the occurrence of the convective clouds that are due to convection from the ground. From this, however, it does not follow that the theories underlying the parcel method and the slice method are capable of accounting for other aspects of convection, such as the vertical velocities, the vertical and horizontal extent of convective clouds, etc. These questions will be examined by the aid of the selected cases to be analysed in the following paragraphs.

It will be seen from the Tables IX and X that of the 174 cases in the categories A and C (which certainly represent convection from the ground), about 75 % occurred without a negative area near the ground, and in about 90 % of the cases were the negative areas less than 0.5 cm². This seems to suggest that *the condition for convection to be released can be expressed by the smallness of the negative area rather than by the difference between the size of the positive and the negative area* (see also paras. 2 and 21).

18. Amount of Convective Clouds.

It was mentioned in para. 4 that the parcel method does not give any information as to the amount of convective clouds that may develop for any given stratification. On the other hand, it was shown in para. 9 that according to the slice method there is, for any given lapse rate, an upper limit to the amount of *energy-producing clouds*. In addition to this amount, energy-consuming clouds may exist, but as long as convection is active, the descending currents around the energy-producing clouds will tend to eliminate the energy-consuming clouds, with the result that in the active phase of the convective process most of the clouds are energy-producing, whereas in the last phase, when the convection is dying out, large masses of passive, or energy-consuming clouds may be present in the sky.

Furthermore, it follows from the slice method that the upper limit for the amount of energy-producing cloud is about 5 tenths, except in rare cases when the lapse rate is excessively steep. On the basis of this, one would expect to find that in the large majority of cases, the amount of cloud is 5 tenths or less.

The percentage frequency of the amounts of cloud of the cumulus type (i.e. Cu and Cb), as reported by the air observers at Bircham Newton and Aldergrove, are given in Table XII, for the selected and the non-selected series of observations.

Table XII.

Percentage Frequency of Amounts of Cloud of the Cumulus Type. Bircham Newton and Aldergrove.

Amount	Non-selected series	Selected series	Mean
Trase or 1/10	16	6	11
1/4	32	24	28
1/2	41	53	47
3/4	8	14	11
9/10	3	3	3
> 9/10	0	0	0
1/2 or less	89	83	86
3/4 or more	11	17	14

It will be seen from Table XII that in about 85 % of the cases was the amount of cumulus and cumulo-nimbus cloud 5 tenths or less. Assuming that, in most of the cases, there are also some amounts of energy-consuming or passive clouds present, it will be seen that the amount of energy-producing cumulus rarely exceeds 5 tenths, which is in good agreement with what the slice method indicates. In this connection it should be noted that the amounts of convective cloud reported by the ground observer will exceed those reported by the air observer by several tenths on account of the perspective effect.

19. Cloud Base.

As shown in paras. 2 and 10, the condensation level is obtained from the surface observation by assuming that the air ascends dry-adiabatically without appreciable mixing with the environment. The condensation levels thus evaluated are independent of the theories underlying the parcel method and the slice method.

The condensation levels have been evaluated from the TePhi-grams (the selected series) and compared with the actually observed cloud bases, and the results are shown in Tables XIII—XVI.

Table XIII.

Comparison between Observed Cloud Base and Computed Condensation Level. Selected Series. All Cases included.

Computed Condensation Level (mb)	Observed Cloud Base (mb) 1000 990	980 970	960 950	940 930	920 910	900 890	880 870	860 850	840 830	820 810	800 790	780 770	760 750	Total
1000—990	0	9	10	2	3	1	2	–	1	–	–	–	1	29
980—970	3	14	12	7	3	5	–	–	–	–	–	–	–	44
960—950	1	4	15	15	9	6	4	1	2	1	–	1	1	60
940—930	–	1	4	13	19	16	7	–	–	3	–	–	1	64
920—910	–	2	3	2	4	8	7	1	3	1	–	–	1	32
900—890	–	–	1	3	1	2	3	4	6	1	1	–	–	22
880—870	–	–	–	–	–	–	1	4	5	2	1	1	–	14
860—850	–	–	–	–	–	–	1	2	4	–	2	1	–	10
840—830	–	–	–	–	–	–	1	–	0	1	–	1	–	3
Total	4	30	45	42	39	38	26	12	21	9	4	4	4	278

Mean Observed Cloud Base ..... = 908 mb
Mean Computed Condensation Level = 938 mb
Difference ..... = –30 mb
Correlation Coefficient ..... = 0.62

Note: Underlined figures indicate the diagonal.

Table XIV.

Comparison between Observed Cloud Base and Computed Condensation Level. Selected Series; only Cases with Showers, Hail and Thunderstorms are included.

Computed Condensation Level (mb)	Observed Cloud Base (mb) 1000 990	980 970	960 950	940 930	920 910	900 890	880 870	860 850	840 830	820 810	800 790	780 770	760 750	Total
1000—990	0	2	5	–	1	–	–	–	1	–	–	–	1	10
980—970	1	6	4	3	1	3	–	–	–	–	–	–	–	18
960—950	–	3	11	7	6	1	2	1	2	1	–	1	–	35
940—930	–	1	2	4	7	2	–	–	–	2	–	–	1	19
920—910	–	2	2	0	2	2	4	1	–	–	–	–	1	14
900—890	–	–	–	1	1	0	1	1	–	–	–	–	–	4
880—870	–	–	–	–	–	–	0	–	–	–	–	–	–	–
860—850	–	–	–	–	–	–	–	1	–	1	–	–	–	2
Total	1	14	24	15	18	8	7	4	3	4	–	1	3	102

Mean Observed Cloud Base ..... = 917 mb
Mean Computed Condensation Level = 950 mb
Difference ..... = –33 mb
Correlation Coefficient ..... = 0.32

Note: Underlined figures indicate the diagonal.

Table XV.

Comparison between Observed Cloud Base and Computed Condensation Level. Selected Series; only Cases with Convective Strato-cumulus, without Precipation and other low Cloud Forms are included.

Computed Condensation Level (mb)	Observed Cloud Base (mb) 1000 990	980 970	960 950	940 930	920 910	900 890	880 870	860 850	840 830	820 810	800 790	780 770	760 750	Total
1000—990	0	2	3	–	–	–	(2)	–	–	–	–	–	–	7
980—970	1	3	5	1	2	–	–	–	–	–	–	–	–	12
960—950	–	1	3	2	1	1	2	–	–	–	–	–	(1)	11
940—930	–	–	–	1	4	6	2	–	–	–	–	–	–	13
920—910	–	–	1	–	1	1	–	–	1	–	–	–	–	4
900—890	–	–	–	–	–	1	–	1	–	–	–	–	–	2
880—870	–	–	–	–	–	–	0	1	–	–	1	–	–	2
860—850	–	–	–	–	–	–	–	0	–	–	–	–	–	0
840—830	–	–	–	–	–	–	1	–	0	–	–	1	–	2
Total	1	6	12	4	8	9	7	2	1	–	1	1	1	53

Mean Observed Cloud Base ..... = 918 mb
Mean Computed Condensation Level = 945 mb
Difference ..... = –27 mb
Correlation Coefficient ..... = 0.72

Note: Underlined figures indicate the diagonal.

Table XVI.

Comparison between Observed Cloud Base and Computed Condensation Level. Selected Series; only Cases with Clouds of Cumulus Type without Precipation and other Low Cloud Forms are included.

Computed Condensation Level (mb)	Observed Cloud Base 1000 990	980 970	960 950	940 930	920 910	900 890	880 870	860 850	840 830	820 810	800 790	780 770	760 750	Total
1000—990	0	4	4	–	2	1	–	–	–	–	–	–	–	11
980—970	–	3	1	4	–	–	–	–	–	–	–	–	(1)	9
960—950	1	1	1	5	2	2	1	–	–	–	–	–	–	13
940—930	–	–	2	4	4	8	3	–	–	1	–	–	–	22
920—910	–	–	1	1	2	4	2	–	–	1	–	–	–	11
900—890	–	–	–	2	1	2	3	3	1	1	–	–	–	13
880—870	–	–	–	–	–	1	3	5	2	–	1	–	–	12
860—850	–	–	–	–	–	1	2	3	1	1	1	–	–	9
Total	1	8	9	16	11	19	14	11	4	4	2	–	1	100

Mean Observed Cloud Base ..... = 902 mb
Mean Computed Condensation Level = 924 mb
Difference ..... = –22 mb
Correlation Coefficient ..... = 0.74

Note: Underlined figures indicate the diagonal.

It will be seen from Table XIII that there is a fair correlation between the computed condensation level and the observed cloud base; but the scatter is appreciable, and there is a systematic difference of —30 mb, showing that the cloud base is normally appreciably higher (approximately 900 ft) than the evaluated condensation level.

An attempt has been made at grouping the observations according to type of cloud, weather,

etc., and the results are shown in Tables XIV—XVI.

It will be seen from Table XIV that, when precipitation is falling from convective clouds, the correspondence is very slight, and there is a clear indication of the cloud base being above (approximately 1000 ft) the computed condensation level. The explanation for this is obvious. The precipitation causes the cloud base to become variable and largely unrelated to the surface conditions. Below the cloud base the air is moistened by the rain, and at the ground the air is moistened also by evaporation from terrestrial sources of water, with the result that the condensation level evaluated from surface observations will give too low values of the heights, and too high values of pressures at the condensation level.

It will be seen from Table XV that, except for the three wild cases indicated by parentheses,[1]) the correspondence is very good; the correlation is 0.72, but there is a systematic difference of —27 mb showing that the base of convective strato-cumulus is appreciably higher (i.e. about 800 ft) than the computed condensation level.

Table XVI shows that the correspondence between computed and observed base of cumulus clouds is very high; the correlation is 0.74 and the mean difference is —22 mb or about 650 ft. It will be seen that the difference does not vary much with the height of the cloud base.

If there were any appreciable mixing between the ascending and descending masses below the cloud base one would expect that the difference between the observed and computed condensation level would increase with increasing distance from the ground to the cloud base, for the ascending air would then gradually mix with the descending air and become increasingly dryer as it ascends. Table XVI, however, shows no appreciable tendency in this direction.

The earth's surface (in the British Isles) being a source of moisture, it is to be expected that the air at the ground will normally contain more humidity than does the bulk of the air below the cloud base. If this is so, the computed condensation level would be too low, for a non-representative saturated-adiabatic would be used in evaluating the condensation level.

During the period to which the observations refer, no detailed observations of temperature and humidity were made within the friction layer, but such observations were initiated later. From 100 ascents made in convective situations at Aldergrove and Bircham Newton in July 1944, the following mean values of the potential wet-bulb temperature were found.

Level (ft)	Potential wet-bulb temperature (°F)
0	56.6
500	55.3
1000	54.8
1500	54.6

It will thus be seen that the normal state in convective situations is characterized by an excess humidity in a relatively shallow layer near the ground and a gradual approach to a representative potential wet-bulb temperature at about 1000 ft above the ground. Using now the representative value 54.6 instead of the surface value 56.6, the condensation level is increased by a height corresponding to a little more than 20 mb, which is sufficient to account for the differences indicated in Table XV and XVI.

Let CB and CL denote the cloud base and the computed condensation level, both expressed in terms of pressures. Then, approximately

$$CB = CL - 25 \text{ (mb)}$$

If this relation is used in connection with the observations in Table XV and XVI, one would obtain the cloud base with an accuracy of $\pm$ 25 mb in about 75 % of the cases; errors of $\pm$ 50 mb would occur only in about 12 % of the cases.

20. Cloud Top.

It was shown in paras. 3 and 4 that the parcel method leads to the result that the top of the convective cloud should reach to the top of the upper negative area, i. e. to the level GF in Fig. 2. Poulter (1938), on the other hand, finds that the convective clouds tend to build up to the top of the positive area, i.e. to the level E in Fig. 2. Other authors contend that nature prefers a compromise between these two levels, which means that the top of the convective cloud would nor-

[1]) These cases, as well as the one Table XVI have been disregarded in the computation of the correlation coefficients and the means.

mally be found somewhere above the top of the positive area and below the top of the upper negative area.

It was shown in para. 9 that the slice method leads to the definite conclusion that the top of the convective cloud would only reach slightly beyond the level D in Fig. 2, i.e. the level where the lapse rate becomes equal to the saturated-adiabatic rate.

Now, if there is active convection below an inversion, the three levels D, E and F in Fig. 2 will approach one another, and the distance from D to E and from E to F will be relatively small. This is almost invariably so in the cases of convective strato-cumulus. In these cases, it is difficult to decide which of the theories renders the most satisfactory results. On the other hand, when convection results in cumulus congestus, or cumulo-nimbus, the distances from D to E and from E to F will be very large and a good check on the validity of the theories can be obtained.

Table XVII.

Percentage Frequencies of Observed Heights of Tops of Cumulus and Cumulo-nimbus and of Similar Heights computed by the Aid of the Slice Method and the Parcel Method. Selected Series. Only Cases of Cu and Cb and with the Level D below 400 mb are included.

Pressure (mb)	Observed cloud top	Computed Height of Cloud Top		
		Slice method i.e. level D	Parcel method, top of upper negative area	Parcel method, top of positive area
< 400	—	—	47	24
400—440	—	—	5	6
450—490	2	2	5	4
500—540	2	1	5	2
550—590	1	4	5	5
600—640	3	2	5	5
650—690	8	2	6	11
700—740	25	6	11	11
750—790	19	28	5	11
800—840	19	23	3	11
850—890	15	20	1	10
900—940	6	12	2	—
Mean	765	790	< 525	< 625
Difference	0	— 25	> 240	> 140

Before we proceed to compare the observed heights of the cloud tops with the computed heights, it is necessary to remark that the ascents under investigation terminate at the 400 mb level, with the result that the levels referred to may escape observation. This is often true of the level F (Fig. 2), which is often found above the 400 mb surface. When this is the case, the levels are tabulated as being at < 400 mb, indicating that the level in question is above the 400 mb surface. The results of these comparisons are given in Tables XVII and XVIII.

It will be seen from Table XVII that the results obtained by the slice method are entirely satisfactory. On the average, the pressure at the level D is 25 mb higher than that at the top of the cloud, which agrees with the findings of the slice method, for the cloud was to penetrate into the stable layer slightly above the level D. In comparison it will be seen that the parcel method renders results that are greatly at variance with the observations. The top of the upper negative area is normally much higher than the top of the convective cloud, and so is also the top of the positive area.

To obtain a more reliable assessment of the accuracies rendered by the methods referred to above, the frequencies of differences in pressure corresponding to Table XVII are given in Table XVIII.

Table XVIII.

Percentage Frequency of Pressure Difference between Computed and Observed Heights of Cloud Tops. Selected Series. Only Cases of Cu and Cb are included.

Pressure Difference (mb)	Level D minus Cloud Top	Level F minus Cloud Top	Level E minus Cloud Top
< — 200	—	61	29
— 200 to — 110	—	17	16
— 100 to — 60	5	10	14
— 50 to — 10	15	7	17
0	20	1	7
10 to 50	47	1	13
60 to 100	6	3	3
110 to 200	7	—	1
> 200	—	—	—
Mean	25	<—240	<—140

It will be seen from Table XVIII that the pressure differences resulting from the parcel method are large on the average, and their distribution is erratic. The slice method, on the other hand, gives a pronounced concentration of the

frequencies at about 25 mb. Let p_D be the pressure at the level D, and p_C the pressure at the top of the cloud. Then, on the average, the slice method gives

$$p_C = p_D - 25 \text{ (mb)}$$

If this formula were used to evaluate the heights of the tops of cumulus and cumulo-nimbus, an accuracy of $\pm$ 25 mb would be obtained in about 55 % of the cases, and an accuracy of $\pm$ 50 mb would be obtained in about 80 % of the cases.

The above results refer to cumulus and cumulo-nimbus clouds. In the case of convective strato-cumulos, there is normally an inversion present in the upper part of the cloud layer. The level D (see Fig. 2) will then normally coincide with the base of the inversion, and the top of the positive area will normally be within the inversion layer. Since, in these cases, the positive area below the inversion is relatively small, the upper negative area will also be small, with the result that the parcel method and the slice method give result that do not differ greatly. Normally, the strato-cumulus layer reaches 20—30 mb into inversion layer.

21. Release of Convection: The Maximum Negative Area.

It was shown in para. 5 that an initial vertical velocity of 7.5 m/sec is required for a unit mass to overcome a negative area of 1 cm² on the TePhi-gram, and even if the negative area of the surface air were as small as 0.18 cm², an initial velocity of 1 m/sec would be required to overcome the buoyancy forces. From this it will be seen that the negative area of the surface air must be reduced to an immeasurable size before energy producing convective currents can be released.

On the other hand, the horizontal temperature distribution is not uniform, and when the representative observations show a small negative area, the negative area is likely to vanish locally, and a positive area may be present in places. Thus, for any given negative area on an ascent curve there is a certain probability for a slight positive area to be present locally. Therefore, as pointed out in paras. 5 and 17, convection is likely to be released as soon as the negative area of the ascent curve reaches a certain value. We shall now endeavour to determine the maximum size of the negative area that will allow convection to be released. To this end, the selected series will be used. The problem is a statistical one, and our aim is to determine the maximum size of the negative area, such that when this value is used, satisfactory results will be obtained in at least 90 % of the cases. In view of the discussion in para. 12 it seems reasonable to allow a margin of 10 % to allow for „wild cases" arising from observational errors.

The cumulus, cumulo-nimbus, and strato-cumulus clouds in the selected series have been correlated with the positive and negative areas, and the results are shown in Table XIX.

Table XIX. Percentage Frequency of Cloud in Combinations of Positive and Negative Areas. Selected Series.

Positive Area (cm²)	Negative Area (cm²)													Total
	0	0.1—0.5	0.6—1.0	1.1—2.0	2.1—3.0	3.1—4.0	4.1—5	6—10	11—20	21—30	31—40	41—50	> 50	
0	–	–	–	0.3	0.3	–	–	0.3	3.2	1.8	2.1	1.1	3.2	12.3
0.1—0.5	3.9	3.9	2.1	1.1	0.3	0.3	–	–	–	–	0.3	–	0.3	12.2
0.6—1.0	2.5	3.2	1.4	0.7	–	0.3	–	–	–	–	–	–	–	8.1
1.1—2.0	8.4	3.2	1.8	0.3	–	–	–	–	–	–	–	–	–	13.7
2.1—3.0	4.9	1.1	–	0.3	–	–	–	–	–	–	–	–	–	6.3
3.1—4.0	6.0	0.3	0.7	–	–	0.3	–	–	–	–	–	–	–	7.3
4.1—5	3.2	1.4	–	–	–	–	–	–	–	–	–	–	–	4.6
6—10	10.5	2.1	–	0.3	0.7	–	–	–	–	–	–	–	–	13.6
11—20	12.3	2.1	1.4	0.3	–	–	–	–	–	–	–	–	–	16.1
21—30	3.9	–	–	0.3	–	–	–	–	–	–	–	–	–	4.2
31—40	1.1	–	–	–	–	–	–	–	–	–	–	–	–	1.1
41—50	–	–	–	–	–	–	–	–	–	–	–	–	–	–
>50	0.3	–	–	–	–	–	–	–	–	–	–	–	–	0.3
Total	57.0	17.3	7.4	3.6	1.3	0.9	0	0.3	3.2	1.8	2.4	1.1	3.5	100
No of Cases:	Category 2: 250							Category 1: 35						285

It will be seen that the clouds fall into two categories, viz.,

1. A group (representing about 12 % of the total number) in the upper right hand corner of the table, which is characterised by a very large negative area and, except in two cases, no positive area at all.

2. A group (representing about 88 % of the total number) in the left hand part of the table which, on the whole, is characterised by the absence of, or a very small, negative area.

Of the 35 cases in category 1, 15 cases occurred with precipitation and a stable layer, or inversion, near the ground; in 7 cases strato-cumulus was reported, and in the remainder of the cases, feeble fronts appeared to be present aloft. In all but 3 of the 35 cases, pronounced instability was found in the upper atmosphere. It is evident that the clouds referred to in category 1 resulted from convection released in the free atmosphere and not from the ground. These cases will therefore be excluded from the following discussion.

Having removed the 35 cases in category 1, there remain 250 cases to be examined.

When precipitation falls, the surface temperature and wet-bulb temperature will often become non-representative as a result of evaporation from terrestrial sources of water. We shall therefore discuss the cases with and without precipitation separately. The cases with precipitation are shown in Table XX.

Table XX.

Percentage Frequency of Cloud in Combinations of Positive and Negative Areas. Selected Series. Only Cases with Precipitation are included.

Positive Area (cm²)	Negative Area (cm²) 0	0.1—0.5	0.6—1.0	1.1—2.0	2.1—3.0	3.1—4.0	4.1—5.0	Total
0	–	–	–	0.4	0.4	–	–	0.8
0.1—0.5	2.0	–	1.2	0.4	–	0.4		4.0
0.6—1.0	1.6	1.2	0.4	0.4	–	–	–	3.6
1.1—2.0	2.4	1.2	0.8	0.4	–	–	–	4.8
2.1—3.0	0.8	0.8	–	–	–	–	–	1.6
3.1—4.0	1.6	0.4	0.4	–	–	–	–	2.4
4.1—5	0.8	0.8	–	–	–	–	–	1.6
6—10	4.4	1.6	–	0.4	0.4	–	–	6.8
11—20	6.8	1.2	1.2	0.4	–	–	–	9.6
21—30	2.4	–	–	0.4	–	–	–	2.8
31—40	1.2	–	–	–	–	–	–	1.2
41—50	–	–	–	–	–	–	–	–
> 50	–	–	–	–	–	–	–	–
Total	24.0	7.2	4.0	2.8	0.8	0.4	–	39.2

Note: The percentage refer to the total number 250 referred to in Table XIX.

Table XXI.

Percentage Frequency of Cloud in Combinations of Positive and Negative Areas. Selected Series. Only Cases with Strato-cumulus without Precipitation and other Low Clouds are included.

Positive Area (cm²)	Negative Area (cm²) 0	0.1—0.5	0.6—1.0	1.1—2.0	2.1—3.0	3.1—4.0	4.1—5.0	Total
0	–	–	–	–	–	–	–	–
0.1—0.5	0.8	2.8	1.4	0.4	–	–	–	5.4
0.6—1.0	1.6	2.0	1.6	–	–	–	–	5.2
1.1—2.0	4.4	1.2	0.8	–	–	–	–	6.4
2.1—3.0	0.8	–	–	–	–	–	–	0.8
3.1—4.0	2.4	–	–	–	–	–	–	2.4
4.1—5	1.2	0.4	–	–	–	–	–	1.6
6—10	1.2	–	–	–	–	–	–	1.2
11—20	1.2	–	0.4	–	–	–	–	1.6
21—30	–	–	–	–	–	–	–	–
31—40	–	–	–	–	–	–	–	–
41—50	–	–	–	–	–	–	–	–
> 50	–	–	–	–	–	–	–	–
Total	13.6	6.4	4.2	0.4	–	–	–	24.6

Note: The percentage refer to the total number 250 referred to in Table XIX.

Table XXII.

Percentage Frequency of Cloud in Combinations of Positive and Negative Areas. Selected Series. Only Cases with Cumulus without Precipitation and other Low Clouds are included.

Positive Area (cm²)	Negative Area (cm²) 0	0.1—0.5	0.6—1.0	1.1—2.0	2.1—3.0	3.1—4.0	4.1—5.0	Total
0	–	–	–	–	–	–	–	–
0.1—0.5	1.2	0.4	0.4	–	–	–	–	2.0
0.6—1.0	0.4	–	–	0.4	–	–	–	0.8
1.1—2.0	3.6	0.4	–	–	–	–	–	4.0
2.1—3.0	2.8	0.4	–	0.4	–	–	–	3.6
3.1—4.0	2.0	–	0.4	–	–	0.4	–	2.8
4.1—5	–	0.4	–	–	–	–	–	0.4
6—10	5.6	0.8	–	–	–	–	–	6.4
11—20	4.4	0.4	0.4	–	–	–	–	5.2
21—30	1.6	–	–	–	–	–	–	1.6
31—40	0.8	–	–	–	–	–	–	0.8
41—50	–	–	–	–	–	–	–	–
> 50	0.4	–	–	–	–	–	–	0.4
Total	22.8	2.8	1.2	0.8	–	0.4	–	28.0

Note: The percentage refer to the total number 250 referred to in Table XIX.

In order to obtain a reliable assessment of the maximum negative area compatible with convection, we shall eliminate the cases of mixed skies, and discuss separately the cases of convective strato-cumulus and cumulus. Table XXI refers to the cases of convective strato-cumulus without other low cloud forms, and Table XXII refers to the cases when cumulus and no other cloud forms were observed.

1. *Precipitation.* It will be seen from Table XX that, in the majority of the cases, there is no negative area, but there is a fair number of cases with relatively large negative areas; in about 20 % of the cases is the negative area larger than 0.5 cm².

2. *Convective strato-cumulus.* Here, too, (see Table XXI), the negative area is most frequently absent; in about 19 % of the cases is the negative area larger than 0.5 cm², and in less than 2 % of the cases does the negative area exceed 1 cm².

3. *Cumulus.* Table XXII shows a much greater preference for the small negative areas than do the other tables. It will be seen that in about 81 % of the cases is there no negative area, and in 91 % is the negative area 0.5 cm² or less.

Allowing a margin of about 10 % for observational errors, it seems safe to conclude that *cumulus clouds resulting from convection from the ground are not likely to form until the negative area has been reduced to about 0.5 cm².*

It will be seen from Table XXI that, within the same margin of error, convective strato-cumulus may be present even when the negative area slightly exceeds 0.5 cm².

Adopting 0.5 cm² as a convenient upper limit of the negative area that is compatible with convection from the ground, and making no allowance for observational errors, the above tables indicate the following success:

All cases	84 %
Convection with precipitation	80 %
Sc without precipitation and other low clouds	81 %
Cu, or Cb without precipitation and other low clouds	91 %

22. Release of Convection: Diurnal Heating.

We shall now return to the discussion in para. 10 and try to determine the success that can be obtained in the forecasting of convective clouds due to diurnal heating by evaluating the convection temperature T_C, the maximum temperature T_M, and the corresponding condensation levels B and B′, as shown in Fig. 6.

To test the methods suggested in para. 10, the selected series of observations has been used. In order to eliminate all cases of advective heating or cooling, only ascents satisfying the following conditions were used:

(1) No convective cloud present at the time of the morning ascent, but cumulus or cumulonimbus present at the time of the midday ascent (i.e. 1200 GMT).
(2) Wind at station level force 3, or less.
(3) No appreciable change in the temperature at and above the 800 mb surface from morning to midday.

Only 32 ascents were found that satisfied all these requirements. Although the number is small, the results ought to be highly representative of diurnal convection.

For the evaluation of the convective temperature and the condensation level, the surface humidity is of great importance. In evaluating the representative humidity, the method suggested in para. 10 was used, i.e. the mean value through the layer up to the 950 mb surface was evaluated from the TePhi-grams. By the aid of this value the condensation level B and the convection temperature T_C (see Fig. 6) were evaluated.

Next, the appropriate areas (A) given in Table D (para. 10) were applied to the morning ascents, and the maximum temperature (T_M) and the condensation level (B′) (see Fig. 6) were evaluated. Finally, the surface temperature (T_O), the observed cloud base (B_O) at the time of the midday ascent, and the area (A_O) gained from the morning to the midday ascent were evaluated and compared with the theoretical values.

The ratio of the observed area to that given in Table D is given in Table XXIII.

Table XXIII.

Percentage Frequency of the Ratio A_O to A.

Ratio	0.1	0.2	0.3	0.4	0.5	0.6	0.7	0.8
Frequency	6	25	16	19	13	12	3	6

Mean ratio 0.4

It will be seen that the observed areas are much smaller than the values indicated in Table D. It should be noted that the areas in Table D refer to the time of maximum temperature, and should, therefore, on the average, be larger than the areas observed at the time of the midday ascent, i.e. 1200 GMT. Nevertheless, the ratios given in Table XXIII seem to suggest that the areas given in Table D are definitely too large, since more than 40 % of the available energy must have been supplied by 1200 local time.

We shall next consider the evaluated temperatures T_M and T_C. Table XXIV shows the frequencies of the difference between the temperatures observed at 1200 GMT and T_M and T_C, respectively.

Table XXIV.

Percentage Frequency of Differences T_O—T_M *and* T_O—T_C.

Difference (°F)	T_O—T_M	T_O—T_C
< —9	–	6
—9 and —8	–	–
—7 and —6	6	3
—5 and —4	25	6
—3 and —2	22	19
—1 to +1	25	16
2 and 3	13	13
4 and 5	9	22
6 and 7	–	9
8 and 9	–	–
> 9	–	6
Mean	—4	+2

It will be seen that the maximum temperatures, evaluated as described in para. 10, are about 4 °F higher than the temperatures observed at 1200. This difference is altogether reasonable, and since the range of the differences T_O—T_M is fairly small, it appears that Gold's method of forecasting the maximum temperature gives results that are largely satisfactory.

The fact that Gold's method renders satisfactory values for T_M while the areas used are too large, can be explained by reference to Fig. 6. Thus, if the lapse rate above the ground is superadiabatic, instead of adiabatic, a smaller area would give the same value for T_M. Furthermore, if the line MM in Fig. 6 is moved a distance corresponding to 1 °F, the area will vary in proportion to its size. Thus, T_M becomes rather insensitive to an error in the area when the area is large, but it is highly sensitive to such errors when the area is small.

It will be seen from Table XXIV that, on the average, the temperature observed at 1200 GMT is about 2 °F higher than T_C. This is what one would expect, since convection was actually released by 1200 GMT. However, in about 35 % of the cases, convection had been released although the surface temperature had not reached the critical value. The reason for this may, in part, be due to the circumstance that convection is released over over-heated localities before the representative temperature reaches the critical value. This question was discussed in some detail in para. 21.

It will be seen from Table XXIV that the range of the variation in T_O—T_C is appreciable. The extreme cases were found to occur when the ascent curve was irregular near the earth's surface. Furthermore, when the lapse rate in the morning is such that the temperature curve is parallel to the lines of humidity mixing ratio, the intersection is poor, and great errors in the evaluated T_C will result.

It will be seen from Fig. 6 that the point B represents the level at which convective clouds would begin to form, assuming that the humidity mixing ratio remains sensibly constant. On the same assumption, and using Gold's areas, the condensation level at the time of maximum temperature would be found at B′. The levels B and B′ have been evaluated and compared with the height of the base of the convective cloud, and the results are shown in Tables XXV and XXVI, where B_O refers to the observed cloud base.

Table XXV.

Percentage Frequencies of B_O—B′.

Difference (mb)	Cloud base (mb)			
	Below 950	950—910	900—860	Above 860
< —60	–	–	–	–
—60 and —50	–	–	–	3
—40 and —30	–	–	–	3
—20 and —10	–	–	9	–
0	–	–	6	–
10 and 20	–	3	6	–
30 and 40	–	6	9	–
50 and 60	3	9	6	3
> 60	22	9	–	–
Mean without regard to sign 48 mb				
True mean 39 mb				

Table XXVI.

Percentage Frequencies of B_0—B.

Difference (mb)	Cloud base (mb)			
	Below 950	950—910	900—860	Above 860
< — 60	–	–	6	6
— 60 and — 50	–	–	3	–
— 40 and — 30	–	3	13	–
— 20 and — 10	3	6	0	–
0	0	3	3	–
10 and 20	9	3	3	–
30 and 40	3	6	3	3
50 and 60	0	6	0	–
> 60	9	–	6	–
Mean without regard to sign 44 mb				
True mean		6 mb		

It will be seen from Table XXV that the condensation levels obtained by the aid of the areas in Table D are, on the average, much too high, i.e. they occur about 40 mb above the observed cloud base. This suggests that the areas in Table D are too large.

It will also be seen that the error is large (i.e. > 60 mb) when the cloud base is low, and it decreases as the height of the cloud base increases. The reason for this can be explained by reference to Fig. 6. Suppose that the ascent in the morning showed a ground inversion. The point A would then be to the left of the position indicated, and there would be a maximum of temperature at some distance above the ground. To compensate for the area due to the ground inversion, the line MM would only have to be moved slightly downwards, with hardly any effect on the level B′. Thus, the level B′ is rather insensitive to the structure of the air above the ground.

Suppose next that the humidity mixing ratio were considerably higher than indicated in Fig. 6. The line CB would then be found further to the right. But when this occurs, the distance from B to B′ would increase rapidly, depending upon the lapse rate in the air column. Thus, when the condensation level is low, the level B′ will normally be much too high. If, on the other hand, the humidity were less than that indicated in Fig. 6, the line CB would be found further to the left, and the level B′ would be representative.

From the above discussion, it follows that the area method is not suitable for evaluating the condensation level of convective clouds.

It will be seen from Table XXVI that, on the average, the level B agrees well with the observed cloud base, but the scatter is very large, and the error varies with the height of the cloud base. Thus, neither of the two methods of predicting the cloud base at noon by the aid of the morning ascents, give satisfactory results. The errors in the level B are mainly due to the complexities of the ascent curves, and to the poor intersections that are obtained when the ascent curve AB becomes parallel to the humidity curve CB. Appreciable errors are also found when the humidity distribution along the vertical is irregular, and also when the ground is so wet that the dew point varies appreciably as the heating progresses.

To improve on the methods of forecasting the condensation level, the convective temperature and the maximum temperature, more accurate assessments of the available energy, and of the transfer along the vertical of heat and moisture, would be needed.

23. Equivalent Cloud Amount.

It was shown in para. 21 that whether or not convection will occur depends upon the size of the negative area. The size of the positive area appears to be related to the amount of convective cloud, but this relationship is not apparant if the positive areas are compared with the cloud cover, i.e. the number of tenths of the sky covered by cloud, for when the positive area is small, there is usually an inversion above the unstable layer, and convection will then tend to produce a thin layer of cloud that covers a large portion of the sky. However, if the cloud cover and the depth of the cloud are converted into equivalent cloud amounts, as explained in para. 17, the relationship shown in Table XXVII is found.

Table XXVII.

Equivalent Cloud Amounts. Non-selected Series Only Cases with Cumulus or Cumulo-nimbus are included.

Positive Area (cm^2)	Mean Equivalent Cloud Amount	Number of Cases
0.1— 1.0	3	35
1.1— 3.0	4	26
3.1—10.0	9	32
11.0—20.0	19	16
> 20	13	10

It will be seen from Table XXVII that, on the average, there is an almost linear relation between the size of the positive area and the equivalent cloud amount, but the scatter of the individual values around the mean has been found to be appreciable.

24. Release of Precipitation.

As mentioned in para. 13 there is reason to believe, that the presence of ice-crystals and super-cooled water in the clouds is a necessary condition for the release of precipitation of the intensity, that is normally observed in connection with convective clouds[1]). It was also pointed out that the depth of the cloud is an important factor.

In the selected series, 99 cases of precipitation occurred where the temperature at the top of the cloud and the depth of the cloud layer could be evaluated. Of these, 6 observations showed light showers with temperature above freezing at the top of the cloud. In 5 cases light drizzle was reported from strato-cumulus with temperature above freezing at the top of the cloud. In 2 cases it was doubtful whether the light rain reported fell from convective clouds or from an alto-stratus deck present at higher levels.

The remaining 86 cases, in which the temperature at the top of the cloud was below freezing, have been grouped according to temperature intervals and depth of the cloud layer, and the results are shown in Table XXVIII.

The number of cases in each square of the main body of the table is too small for reliable probabilities to be obtained, but the probabilities in the right hand column and in the bottom row are derived from a sufficient number of cases to give significant values. It will be seen that the probability of release of precipitation increases uniformly with decreasing temperature below freezing. It will also be seen that the probability increases rapidly with increasing cloud depth, and when the cloud depth exceeds 300 mb, the probability of precipitation is 80 per cent. It appears, therefore, that a large cloud depth is at least as important as is a sub-freezing temperature in the cloud. It

[1]) It is generally recognised that this condition need not be satisfied for the release of droplets of the drizzle size.

Table XXVIII.

Percentage Probability of Precipitation in Combinations of Temperature at the Top of the Cloud and Depth of Cloud Layer. Selected Series.

Depth of Cloud Layer (mb)	Temp. (°F) at Top of Cloud				Number Cases with Precipitation	Number of Cases without Precipitation	Probability %
	32–28	27–23	22–18	< 18			
< 50	14	40	0	40	4	20	17
60—100	1	17	50	29	6	22	21
110—150	0	29	40	29	6	18	25
160—200	13	22	60	36	10	24	29
210—300	33	30	75	59	17	17	50
> 300	33	–	–	82	43	11	80
Number of Cases with Precipitation	6	10	10	60	86	–	–
Number of Cases without Precipitation	39	27	11	35		112	–
Probability%	13	27	48	63	–	–	43

should be emphasized that the probabilities indicated above refer to the occurrence of precipitation at the time of observation. If the temperature and the cloud depths had been correlated with the occurrence of precipitation within a time interval, say 3 hours, substantially higher probabilities might have been found.

From the above discussion it follows that observations seem to substantiate Bergeron's theory for colloidal instability. The few cases, mentioned at the beginning of this paragraph, in which precipitation fell from clouds without the temperature in the cloud being below freezing, do not necessarily contradict the theory, for drops of drizzle dimensions are normally released without the assistance of ice crystals.

25. The Lapse Rate within Convective Cloud.

The selected series has been used to evaluate the lapse rate that normally occurs within convective clouds. Observations are made at intervals of 50 mb. The evaluated lapse rate will, therefore, represent mean values through relatively deep layers. Particularly when the convective currents are strong, the observing aircraft prefers to fly between the clouds, with the result that the cases of ascents through convective clouds are relatively rare, and will not contain

cases of intense convection. On account of this, and because of the smoothing over 50 mb layers, lapse rates considerably larger than those indicated below are likely to occur.

It is convenient to compare the lapse rate within the cloud with the saturated-adiabatic rate at the appropriate pressure and temperature. In the notations used in the foregoing paragraphs, the *excess lapse rate* is defined as

$$\gamma - \gamma_s$$

Since the saturated-adiabatic lapse rate varies with pressure and temperature while the dry-adiabatic lapse rate is constant, it is convenient to express the excess lapse rate as a percentage of the dry-adiabatic rate. Thus

$$\gamma_E = 100 \frac{\gamma - \gamma_s}{\gamma_d}$$

When the excess lapse rate is positive the cloud is unstable, and when it is negative the cloud is stable.

The excess lapse rates (γ_E) derived from the selected series, are given in Table XXIX.

Table XXIX.

Percentage Frequency of Excess Lapse Rates expressed as a Percentage of the Dry-adiabatic Rate. Selected Series. Total Number of Cases 63.

γ_E (%)	Pressure (mb)			Total
	> 800	800—600	600—400	
< — 20	1.5	3.0	1.5	6.1
— 20 to — 11	3.0	1.5	1.5	6.1
— 10 to — 1	1.5	1.5	3.0	6.1
0	7.6	10.6	3.0	21.2
1 to 10	9.1	3.0	3.0	15.2
11 to 20	6.1	9.1	15.1	30.2
21 to 30	9.1	1.5	–	10.6
> 30	3.0	1.5	–	4.5
Total	40.9	31.8	27.2	100.0
Stable	6.1	6.1	6.1	18.3
Neutral	7.6	10.6	3.0	21.2
Unstable	27.3	15.1	18.1	60.5

It will be seen from Table XXIX that instability within the cloud mass is a very frequent occurrence. It is of interest to note that in 5 per cent of the cases was the lapse rate within the cloud equal to the dry-adiabatic rate, and in 10 per cent of the cases did it exceed that rate. The largest excess lapse rate was 43 per cent of the dry-adiabatic rate.

26. Vertical Velocity and Gusts.

We shall now endeavour to assess the order of magnitude of the vertical velocities and accelerations in the convective currents by applying the theories of convection to the observed temperatures, lapse rates and humidities. The accuracy that can thus be obtained will depend greatly on the underlying assumptions. We shall apply the theory first to saturated ascent through a dry environment (i.e. cloud versus cloudless air), and then to saturated ascent through a saturated environment (i.e. vertical gusts within the cloud).

1. *Saturated ascent through a dry environment.* As shown in paras. 2 and 3, the parcel method leads to the result that the maximum vertical acceleration occurs at the level D in Fig. 2, and the maximum vertical velocity at the level E. It was shown in para. 5 that the vertical velocity at the level E would be proportional to the square root of the positive area below that level. These areas have been evaluated from the ascent curves and converted into velocities, using Table C in para. 5. The results are shown in Table XXX.

Table XXX.

Percentage Frequency of Vertical Velocities at the Top of the Positive Area, or at the 400 mb. Level if the Positive area extends beyond that Level. Selected Series.

w (m/sec) (calculated)	Clouds of cumulus type	Strato-cumulus
0.1—1.0	–	–
1.1—2.0	1	3
2.1—3.0	2	7
3.1—4.0	4	5
4.1—5.0	3	7
5.1—10	19	47
11—15	17	13
16—20	13	8
21—25	13	7
26—30	13	3
31—40	10	–
41—50	4	–
> 50	1	–
Total	100	100
Mean Velocity	19 m/sec	10 m/sec

It will be seen that these velocities bear no resemblance to observed facts. Thus, according to Table XXX, the mean vertical velocity at the top of the positive area would be about

20 m/sec in cumulus situations, and 10 m/sec in strato-cumulus situations. These velocities would represent the mean values for the entire mass of saturated air. On the other hand, it was shown in para. 7 that the parcel method, when applied to saturated ascent through a dry environment, leads to a very great overestimate of the available energy, and, hence, the velocities given in Table XXX will be much too large.

It was shown in para. 8 that the ascending velocity of the saturated air as a whole, relative to the non-saturated environment, must normally be considerably less than 1 m/sec, and it was shown in para. 20 that the vertical velocity and acceleration of the ascending cloud mass are usually nullified more than 100 mb below the level E in Fig. 2, where the parcel method leads to mean vertical velocities of gale force. In view of this, the values given in Table XXX must be discarded as having no foundation in re[1]).

2. *Vertical gusts within the cloud.* It was shown in paras. 6, 7 and 9 that the parcel method leads to an underestimate of the available energy when both the ascending and the descending masses follows the same adiabatic. The underestimate of the available energy is proportional to the factor M'/M, and if the ascending and the descending masses are about equal, the parcel method will give only about 50 per cent of the true amount of energy.

Below the cloud base the lapse rate is only slightly super-adiabatic through a relatively shallow layer, and the positive area will be small, with the result that the vertical gusts are not excessive.

Within the cloud, the conditions are different, for when the rising air reaches the condensation level with a lapse rate that is almost dry-adiabatic, a very large positive area becomes immediately available and strong gusts will occur. If no mixing occurred between the ascending bubbles and their environment, excessive velocities would result. Mixing, however, will smooth out the temperature contrasts, and the velocities that result will depend largely upon the lapse rate within the cloud and the life of the bubbles.

To obtain an assessment of the vertical gusts within the cloud, we shall use the lapse rates given in Table XXIX. We shall assume that the ascending bubble within the cloud is sufficiently large to maintain its identity while it ascends through a layer 50 mb deep.

As pointed out in para. 25, the lapse rates given in Table XXIX do not represent maximum values, for (1) they have been smoothed over a 50 mb layer, and (2) the observing aircraft will avoid extreme conditions.

The lapse rates given in Table XXIX have been converted into the accelerations and velocities that would obtain when a bubble has moved through a layer 50 mb deep. The results are shown in Table XXXI and XXXII.

Table XXXI.

Percentage Frequency of Vertical Accelerations after Passage through a 50 mb Layer, derived from the Lapse Rates in Table XXIX. Only Cases of Instability are included.

Acceleration (m/sec²)	Level (mb)			Total
	Below 800	800—600	600—400	
0.01	10.0	2.5	–	12.5
0.02	10.0	7.5	5.0	22.5
0.03	5.0	5.0	2.5	12.5
0.04	15.0	5.0	22.5	42.5
0.05	–	2.5	–	2.5
0.06	5.0	2.5	–	7.5
Total	45.0	25.0	30.0	100.0

It will be seen that the accelerations are very small. Even if the bubble ascended through a 100 mb layer without loss of excess temperature, the accelerations would only be twice as large

[1]) An attempt has been made at applying the theory of the so-called virtual mass to bubbles of air ascending through the atmosphere (cfr. Lamb. Hydrodynamics, paras. 110—114). According to this theory, the velocity of the ascending bubble is reduced by a factor which depends upon the shape of the bubble, the reduction being due to the circumstance that part of the available energy is used to create compensating currents in the environment. Reduction factors to be applied to the vertical velocities obtained by the aid of the parcel method have been computed for ellipsoids of various eccentricities. It was found that the reduction factor varied from 0.50 to 0.97 as the ratio of the axes varied from 0.2 to 5.0. For a sphere the reduction factor is 0.82. It will thus be seen that the computed reduction factors are unable to account for the excessive velocities shown in Table XXX. The computations show that the theory of the virtual mass for an ideal fluid has but little bearing on convection in the atmosphere.

as indicated in the table, and if the excess lapse rate, in extreme cases, should be twice as large as the steepest one contained in Table XXIX, the acceleration would be twice as large as the largest one in the above table. It appears, therefore, that accelerations in excess of 0.25 m/sec^2 are extremely unlikely even in the most active cumulo-nimbus cloud.

With regard to the vertical velocities of the gusts within the cumulo-nimbus clouds, similar considerations hold. According to Table XXXII, vertical gusts of 6 m/sec should be a fairly frequent occurrence in convective clouds that reach above the 600 mb surface. Allowing, as above, for a longer life of the individual bubbles and lapse rates that occasionally are steeper than the steepest one contained in Table XXIX, gust velocities in the vicinity of 20 m/sec might be reached in extreme cases.

Table XXXII.

Percentage Frequency of Vertical Velocities after Passage through a 50 mb Layer, derived from the Lapse Rates in Table XXIX. Only Cases of Instability are included.

Velocity m/sec.	Level (mb)			Total
	Below 800	800—600	600—400	
1	–	–	–	–
2	10.0	–	–	10.0
3	10.0	7.5	–	17.5
4	15.0	7.5	7.5	30.0
5	10.0	7.5	5.0	22.5
6	–	2.5	17.5	20.0
Total	45.0	25.0	30.0	100.0

With regard to gust gradients within the convective cloud, no deductions can be made from the observational material examined.

27. Relation to Synoptic Situation.

The occurrence of convection has been correlated to the synoptic situation, and some of the results obtained were described in para. 15, in order to characterize the selected series of observations. Some additional results are given in the tables below.

1. *Vertical Shear.* The vertical shear of the horizontal wind through the convective layer is usually small. On the average the shear per 50 mb layer from the base to the top of the cloud was found to be 2 km per hour. The shear increases rapidly above the cloud top, the mean shear through the 50 mb layer above the cloud top was found to be 8 km per hour.

The shear is not uniformly distributed through the cloud layer. On the average, there is a slight shear at the cloud base, uniform velocity through the main cloud layer, and increasing shear towards the top of the cloud, with strong shear above the cloud top. Since strong wind shear is indicative of the presence of horizontal temperature gradients, the shear above the cloud suggests that the cloud tops reach up to the first stable layer, in agreement with what was found in paras. 8 and 20.

The frequencies of variation of wind direction through 50 mb layers from the base to the top of the convective cloud, are shown in Table XXXIII.

Table XXXIII.

Percentage Frequency of Variation in Wind Direction: (1) Convection, (2) regardless of Convection, and (3) above Cloud Top.

Degrees	(1)	(2)	(3)
< -30	–	2	1
-30	1	1	1
-20	3	5	1
-10	13	15	20
0	65	46	54
10	14	22	20
20	3	5	3
30	1	2	–
> 30	–	2	–
Max.	30	150	40

It will be seen from Table XXXIII that, in convective situations, the wind directions is very uniform along the vertical.

2. *Vorticity.* It was shown in para. 15 that there was a slight tendency for convection to occur in cyclonically curved sea level isobars. In an earlier paper[1]) it was found that there was a very high association between the occurrence of subsidence and anticyclonic vorticity in the free atmosphere. Since subsidence is a stabilising process it would seem that convection might not readily occur together with anticyclonic vorticity.

[1]) Unpublished.

This point has been examined and the occurrence of convection has been correlated with the curvature and the shear of the flow in the 750 mb surface. The results are given in Table XXXIV.

Table XXXIV.

Percentage Association between the Occurrence of Convection and the Shear and the Curvature of the Flow at the 750 mb Level. Selected Series. All Cases included.

Curvature	Shear			Sum
	None	Cyclonic	Anticyclonic	
None	19	12	4	35
Cyclonic	13	30	5	48
Anticyclonic ..	5	3	9	17
Sum	37	45	18	100

It will be seen from Table XXXIV that the association between convection and cyclonic vorticity is not very high. In 55 per cent of the cases there is cyclonic vorticity, in 18 per cent anticyclonic vorticity, in 8 per cent the vorticity is indeterminate, and in 19 per cent there is neither cyclonic nor anticyclonic vorticity.

We shall now divide the cases into three classes according to the height of the tops of the convective clouds, such that *shallow convection* will refer to the cases where the cloud tops were found at, or below, the 800 mb surface, *deep convection* will refer to the cases where the cloud tops reached to, or above, the 600 mb surface, and *very deep convection* where the cloud tops reached to, or above, the 400 mb surface. Each of these groups has been correlated with the curvature and shear of the flow in the 750 mb surface, and the results are shown in Table XXXV, in which "indeterminate" refers to the cases when the shear and the curvature were of opposite sign.

It will be seen from Table XXXV that there is a slight preference for anticyclonic vorticity aloft when the convection is shallow. In many of these cases it was found that the convection was limited upwards by an inversion, or a stable layer due to subsidence in the upper strata.

It will also be seen that deep and very deep convection is very intimitely associated with cyclonic vorticity. Although the dynamical causes of this association have not been explored, the statistical evidence suffices to indicate that *deep and very deep convection should not be forecast unless the upper air charts show indication of cyclonic vorticity.*

Table XXXV.

Percentage Association between the Occurrence of Convection and the Vorticity of the Flow at the 750 mb Level. Selected Series.

Vorticity	Shallow	Deep	Very deep
Cyclonic	29	85	94
Anticyclonic	41	1	0
Indeterminate	10	1	0
Nil	20	13	6
No. of Cases	96	73	30

28. Some Cases of deep Convection.

Some typical cases of deep convection are listed in Table XXXVI, together with the observations of weather, cloud, etc. The mean values of temperature and wet-bulb temperature are plotted in Fig. 8.

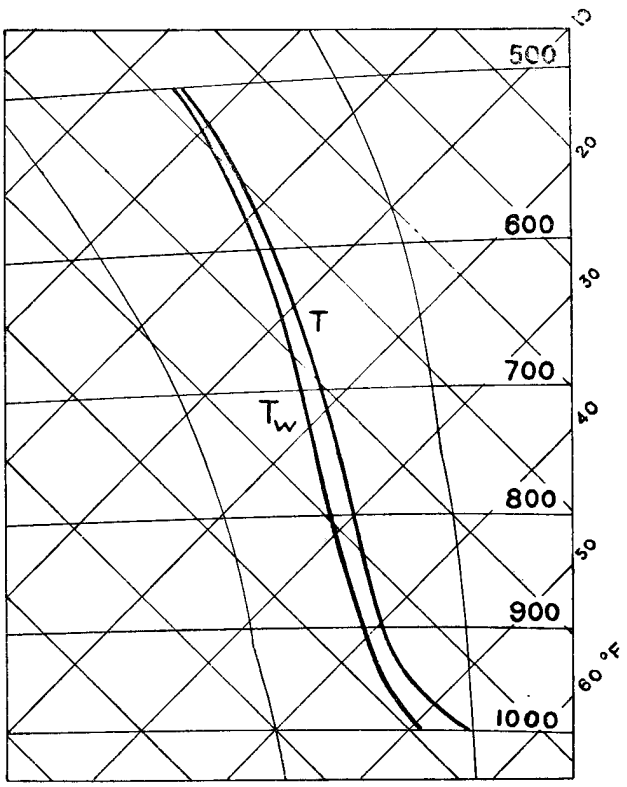

Fig. 8. Mean temperature and wet-bulb temperature in 17 typical cases of deep convection. Two saturated-adiabaties on either side of the ascent curves are indicated. The mean cloud base is at 925 mb. Note the pronounced convective instability above the gronud.

Table XXXVI.

Typical Cases of Convection through a deep Layer. Aldergrove, 1943.

Date	Time	Cloud	Weather	Cloud						Negative Area (cm^2)	Positive Area (cm^2)
				Base (mb)	Top (mb)	Base (°F)	Top[1] (°F)	Amount (tenths)	Equivalent Amount		
May 9	12	Cb, Sc	Hail	950	< 400	35	— 47	5	> 55	0	26
June 12	12	Cb, Cu	Rain showers	970	< 400	50	— 35	5	> 57	0	> 21
» 12	18	Cb, Cu, Sc	Rain showers	970	< 400	51	— 31	3	> 34	0	14
» 14	18	Cb, Cu, Sc	Rain showers	940	470	46	— 20	2—8	29	0	> 10
» 15	12	Cb, Cu	Past showers	960	< 400	46	— 41	3—6	85	0.4	> 7
» 16	12	Cb	Rain showers	940	490	45	— 17	8	72	0	20
July 7	06	Cu, Sc	Rain showers	840	440	33	— 28	8	64	0	> 3
» 12	06	Cb, Sc	Nil	930	500	45	— 15	5	43	0	> 14
» 12	12	Cb, Cu	Rain showers	870	< 400	40	— 34	5	> 47	0	> 16
» 12	18	Cb, Cu	Rain showers	910	430	44	— 29	7	67	0.1	> 16
Aug. 20	12	Cb, Cu	Rain showers	940	410	58	— 17	3—5	54	0	> 16
» 21	18	Cb, Cu, Sc	Rain showers	910	400	52	— 25	6	54	0	> 16
» 25	18	Cb, Cu, Ac	Rain showers	850	< 400	37	— 36	5—8	> 64	0.5	12
» 26	12	Cb, Sc	Nil	920	500	46	— 13	5	42	0.4	> 14
» 26	18	Cb, Cu, As	Past showers	950	420	48	— 30	1—5	16	0	> 15
Oct. 2	12	Cc, Cu	Rain showers	920	450	37	— 30	2—5	23	0	14
Nov. 29	12	Cb, Sc, Ac	Past showers	960	440	36	— 42	3—7	74	0.4	7
			Mean	925	< 432	46	— 29	5	> 52	0.1	> 14

[1] Where the cloud reaches above the 400 mb surface, the temperature refers to the 400 mb surface.

It will be seen that the lapse rate above the ground is slightly super-adiabatic, i.e. there is no negative area. The mean cloud base is at about 925 mb. Below this level, the lapse rate of the wet-bulb temperature exceeds the saturated-adiabatic rate. The air below the cloud base is, therefore, convectively unstable. The same is true, to a lesser extent, from the cloud base to about 750 mb, above which level T_w follows a saturated-adiabatic. The lapse rate of temperature is, however, in excess of the saturated-adiabatic rate throughout, with the result that the cloud will be in an unstable state. Since there is no stable layer below the 500 mb surface, the clouds will build beyond this level.

The convective instability in the lowest strata is an important factor, for when this air rises and becomes saturated, a super-adiabatic lapse rate will be maintained within the cloud, giving rise to strong convective gusts.

It will be seen from Fig. 8 that the wet-bulb depression is positive throughout. This is due to the circumstance that in the majority of the cases, the observing aircraft ascended outside the cloudy columns. However, when the lapse rate outside the cloud is steep, the mean lapse rate within the cloud will also be steep, for, otherwise, excessive temperature contrasts would exist above the cloud tops. It follows then, that a steep lapse rate outside the cloud is indicative of an equally steep lapse rate within the cloud, and the chances for strong gusts to occur within the cloud can be estimated from the lapse rate observed outside the cloud.

Finally, it will be seen from Fig. 8, that the environment of the cloud is in a stable state, for its lapse rate is less than the dry-adiabatic. Within the cloud, on the other hand, the lapse rate is greater than the saturated-adiabatic, with the result that the cloud represents a *chute of instability* through the convective layer. A bubble that ascends from the ground and reaches the cloud base, will become energy-producing, whereas a bubble that ascends from the ground into the air between the cloudy column, will become energy-consuming. Hence, a convective circulation once started, will maintain itself and feed on the bubbles below the cloud while it tends to consume the energy of the bubbles that rise from the ground in the vicinity of the cloud. This state

will continue as long as a super dry-adiabatic lapse rate is maintained above the ground. Hence to maintain convection, the upward transfer of heat through the cloud must be compensated for by a continued heating from the underlying surface. In these circumstances, a considerable portion of the energy areas given in Table D (para. 10) is lost to the upper strata, and this, at least in part, accounts for the absence of agreement between the theoretical and the observed energy areas referred to in para. 22.

SUMMARY

A critical summary of the theories of convection, notably those which lead to the so-called parcel method and slice method of investigating the stability conditions, is given in Section II.

Expressions for the amount of energy, the vertical velocity and acceleration are derived, and the results are compared with Normand's classification of ascent curves. It is shown (1) that both methods lead to consistent criteria for the release of convection from the earth's surface, (2) that the parcel method underestimates the amount of available energy when both the ascending and the descending mass follow the same adiabatic, and (3) that the parcel method greatly overestimates the amount of available energy when saturated air ascends through a dry environment.

The slice method leads to the result that the amount of energy available for the creation of convective currents, depends not only upon the lapse rate of the stratification, but also upon the kinematics of the motion. The slice method, although theoretically sound, is difficult to apply in practice, and in most cases, only qualitative results can be obtained.

The findings of the slice method and of the parcel method are used to obtain assessments of the amount of convective cloud and the height to which the convective cloud will reach. Except when the convection is limited to a shallow layer (i.e. cumulus humulis and strato-cumulus) the two methods give widely different results. Methods of forecasting the convection temperature, the maximum temperature, and the condensation level are discussed in connection with the effective amounts of energy derived by Gold. The use of virtual temperature in the analysis of instability phenomena is discussed, and it is shown that virtual temperature and virtual saturated-adiabatics should be used instead of temperature and ordinary saturated-adiabatics if great accuracy is required. The influence of observational errors is discussed, and the conditions for release of precipitation from convective clouds are summarised.

The theoretical relationships have been compared with actual observations, and the results are discussed in Section III. It is shown that (1) both the parcel method and the slice method give satisfactory criteria to account for the occurrence of convective cloud, (2) while the parcel method gives no information as to the amount of cloud, the slice method gives assessments that are largely in agreement with observations, (3) the base of convective cloud is about 25 mb above the condensation level evaluated from simultaneous observations, but the forecast condensation level is in poor agreement with what is observed, (4) the slice method gives satisfactory results for the heights to which the tops of the convective cloud will reach, whereas the parcel method greatly overestimates these heights.

The release of convective currents from the ground is discussed in considerable detail, and it is shown that convective clouds are likely to appear as soon as the stability of the surface layer is reduced so much that the negative area, as measured on the TePhi-gram[1]), is 0.5 cm², or less. The release of convection caused by diurnal heating is discussed, and it is shown that Gold's method of evaluating the maximum temperature is largely satisfactory, and so is also the method of evaluating the convection temperature, except when the structure of the surface layer is complex.

---

[1]) Form 2810, Meteorological Office, Air Ministry.

The equivalent amount of cloud is introduced to take account of the horizontal as well as the vertical extent of the clouds, and it is shown that this amount is, on the whole, proportional to the available energy.

The probability of release of precepitation is found to increase (a) with the temperature below freezing at the top of the cloud, and (b) with the depth of the cloud.

The lapse rate of temperature within convective cloud is tabulated and discussed in connection with gusts and accelerations. Although the accelerations are very small, vertical gusts in the vicinity of 20 m/sec are likely to be found in the most active cumulo-nimbus.

The occurrence of convection has been correlated with the vertical wind shear and also with the vorticity of the large scale currents at the 750 mb level. The observations show that while shallow convection is unrelated to the vorticity in the free atmosphere, there is a very high association between the occurrence of deep convection and cyclonic vorticity.

Some typical cases of deep convection are tabulated, and their characteristics discussed.

REFERENCES TO LITERATURE

Bergeron, T.	1933.	Memo. Met. Assoc. U. G. G. I.
Bjerknes, J.	1938.	Quart. J. Roy. Met. Soc. *64*, p. 325.
Douglas, C. K. M.	1920.	M. O. Prof. Notes No. 8.
Gold, E.	1933.	M. O. Prof. Notes No. 63.
Hertz, H.	1884.	Met. Zeitschr. Bd. I, p. 421.
Houghton, H. G.	1939.	Physics, Vol. 4, pp. 419—424.
Lord Kelvin.	1865.	Collected Papers, Vol. III, p. 255. (Manchester Phil. Soc. 1865.)
Normand, C. W. B.	1938.	Quart. J. Roy. Met. Soc. *64*, p. 47.
Petterssen, S.	1939:	Geof. Pub. Vol. XII, No. 9.
Petterssen, S.	1940:	Weather Analysis and Forecasting. New York.
Petterssen, S.	1941.	J. Aero. Sc. Vol. 8, No. 3.
Poulter, R. M.	1938.	Quart. J. Roy. Met. Soc. *64*, p. 277.
Refsdal, A.	1930.	Geof. Pub. Vol. V, No. 12.
Rossby, C.-G.	1932.	Papers in Phys. Oceanography and Meteorology, Vol. I, No. 3.
Stüve, G.	1922.	Arb. Aeronaut. Obs. Lindenberg.
Swinbank, W. C.	1944.	Unpublished.

ERRATUM: Sir Charles Normand has drawn the attention of the authors to an error in Table XVII. The frequencies in the pressure interval 900 — 940 mb in the last two columns are inconsistent. As the original manuscript has not been preserved, it is now not possible to correct the error. The inconsistency is regarded as a minor one, and does not affect the general conclusions drawn.

Printed 15th April 1946.

GRØNDAHL & SØNS BOKTRYKKERI. OSLO